Nushagak District Test Fishery, 2019 and 2020

Final Report

BBSRI

Bristol Bay Science and Research Institute
Dillingham, AK 99576

March 1, 2021

Nushagak District Test Fishery, 2019 and 2020

Final Report

Prepared by

Scott W. Raborn[1] and Michael R. Link[2]

Prepared by

Bristol Bay Science and Research Institute
P.O. Box 1464
Dillingham, AK 99576
www.bbsri.org

March 2021

[1] LGL Ecological Research Associates, Inc., 4103 S Texas Ave., Suite 211, Bryan, TX 77802
[2] Bristol Bay Science and Research Institute, P.O. Box 1464, Dillingham, AK 99576

Please cite as:

Raborn, S. W. and M. R. Link. 2021. Nushagak District Test Fishery, 2019 and 2020. Report prepared by the Bristol Bay Science and Research Institute. Dillingham, Alaska. 37 pp.

Available online: www.bbsri.org/

EXECUTIVE SUMMARY

This report presents the results from the Nushagak District Test Fishery for both the 2019 and 2020 seasons. The main body of the report describes the objectives, methods, and results for 2019. The objectives and methods remained unchanged for the 2020 test fishery; as such, we simply update the results for 2020 in Appendix B. We summarize both years as follows.

2019 Season

The purpose of the 2019 Nushagak District test fishery was focused on assessing the early, fishable Sockeye Salmon *Oncorhynchus nerka* abundance in the district to reduce the possibility of a very large passage of fish into the escapement early in the season. As such, the test fishery occurred where the commercial fishery takes place. A secondary motivation for this project was to estimate contact selectivity curves for gillnets in the commercial fishery. Selectivity curves can be used to identify mesh sizes that will optimize the fleet's effectiveness at exploiting harvestable surpluses from the district's river-specific stocks.

A total of 92 sets were made in the Nushagak District from June 15 to July 7 resulting in a total catch of 6,680 Sockeye (49% or 3,283 fish were measured for length). Three different configurations for nets comprised of 4½" and 5⅛" meshes were used varying in total net length and individual shackle length. An additional configuration was used during the middle of the commercial fishery whereby the 5⅛" mesh was replaced with 4¾" mesh.

Despite the exploratory nature of selecting station locations, test fishing catch-per-unit-effort (CPUE) appeared to track the buildup of fish in the district during June 15-21. Likewise, the daily estimates of the Sockeye:Chinook ratio in the test catches seemed to follow that estimated for the reconstructed runs in the District. After June 21, high commercial fishing effort (overall exploitation rate=0.83) was used to prevent/minimize over-escapement into the three systems from a total Nushagak District run of 17.8 million Sockeye. Seasons 2019 and 2018 are good examples of years when escapement was not overly front loaded at the beginning and was spread proportionately throughout the season. However, early runs (2+ days) such as 2003, 2011, and 2013 or very small runs, e.g. 2012, can cause a disproportionate total of the escapement to occur before commercial fishing begins. For instance, in 2013 40% of the escapement had occurred by June 22 compared to only 4% of the catch through that date. The value of a test fishery cannot be determined by a single season outcome, but instead across many seasons, including those when the run behaves unexpectedly.

Estimated selectivity curves for 4½" and 5⅛" meshes under the commercial fishing (CF) protocol showed peak selectivity for the 4½" mesh occurred across the size range for ocean-age 2 fish while that for the 5⅛" mesh occurred over ocean-age 3 fish lengths. However, the relative selectivity differentials were not the same; that is, the 4½" mesh was more selective for ocean-age 3 fish than the 5⅛" mesh was for ocean-age 2 fish. This finding has important ramifications for estimating mesh sizes that optimize catch efficiency (see below).

Two approaches were used to verify that the CF 4½"-5⅛" curve was an accurate representation of gillnet contact selectivity during a commercial opener; both approaches suggested that it was. One of which was to assess how observed catch percentages for the 4½" mesh compared to those predicted from the selectivity curves. During openers when the 4½"-5⅛" mesh pairing and CF protocol was used, we observed that 65% of the catch came from the 4½" mesh—five percentage points greater than our prediction of 60%. Likewise, the observed 4½" catch percentage of 56% for the 4½"-4¾" pairing was five percentage points greater than our prediction of 51%, which also occurred during openers. In other words, we underpredicted the advantage that the 4½" mesh would have over two different larger meshes by a consistent amount during openers. One explanation could be that our predictions were based on the LFD for the entire run and not representative of the LFD that existed in the District during openers when larger fish were likely filtered by the commercial fishery, thereby giving the 4½" mesh an even larger advantage. One would expect then that the observed 4½" catch percentage during closures, when the run was unfiltered by the fishery, would be closer to our prediction. The observed percentage of 59% was closer to the prediction of 60% during closures when the TF protocol and 4½"-5⅛" pairing was used.

The observed size selectivity by the fishery appeared to be dome shaped and more consistent across a wider range of fish sizes than any particular individual mesh size. Across all fishermen, a range of mesh sizes was used which explains why this observed pattern occurred; anecdotal conversations with various fishermen indicated that during 2019, mesh sizes ranged at least from 4½" to 5⅛".

Once the general shape of the selectivity curve was estimated based on the CF 4½"-5⅛" dataset, a curve for any mesh size could be approximated (i.e., in addition to the two meshes used to estimate the curve). We simulated changing mesh size from 4½" to 5⅛" by ⅛" increments and report the hypothetical performance of three objective functions: (1) maximize total catch, (2) maximize total lbs of catch, and (3) equalize exploitation rates across ages. In addition, two simulated runs comprised of 70% 3-ocean and 30% 3-ocean fish were created, and mesh size performances were re-estimated for the same objective functions. The same length frequency distributions (LFDs) for each age were assumed for each simulated run.

The observed run was about evenly split between 3-ocean (48%) and 2-ocean (52%) fish. The mesh size that maximized total catch and equalized exploitation rates was estimated to be 4½", while the 4⅝" mesh was estimated to maximize total lbs of catch; interestingly the average mesh size estimated for the fishery was 4⅝". Had the run been 70% 3-ocean fish, slightly larger meshes would have been more effective to maximize total catch (4¾" mesh) and total lbs (4⅞" mesh). A 30% 3-ocean run would have had all three objective functions optimized with 4½" mesh. Because identical age-specific LFDs were assumed for the observed and simulated runs, it makes sense that 4½" mesh was estimated to equalize exploitation rates for all three scenarios.

Some additional results are noteworthy. First, 4⅝" mesh performed well even when the run's age composition was shifted towards and away from 3-ocean fish (i.e., 70% and 30% 3-ocean runs, respectively). That is, exploitation was more even between the two ocean ages without giving up too much efficiency in maximizing total lbs of catch. The consequence of this finding is that potential evolutionary changes incurred from artificial selection by the fishery could be removed without loss of profits.

Secondly, 5⅛" mesh performed poorly in these regards even when the age composition was shifted towards 3-ocean fish. Catch efficiency for the 5⅛" mesh was the lowest across the range of meshes for all scenarios. This mesh size has been the predominant mesh used historically and has lingered in the fishery perhaps as a carryover from the regulations and/or processors encouraging this larger mesh to increase average individual sizes for when processing capacity was more limiting.

Our results indicate that greater catches can be achieved with mesh sizes smaller than conventional wisdom would lead us to believe. Of course, the overall seasonal catch would not increase from optimizing mesh sizes because specific openings/closures are determined based on escapement counts. Rather, the total time for openings would be reduced to counter this increased efficiency in the fishery.

Future Work Recommendations and Management Implications of the Selectivity Results

- The value of the 2019 Nushagak test fishery for improving management efficiency was marginal as the run was large and more-or-less-continuous openers began early in the season. This utility should increase in years with early and/or small runs.
- Standardizing the net configuration and stations fished in future years should improve the correlation between test fishing CPUE and fish buildup in the District. A 150-fathom net with 25-fathom shackles of alternating mesh worked well to better randomize exposure of individual schools of fish to each mesh size. Continued exploration of station locations should continue for at least one more year before fixed station sites are established. Finally, target mean fishing times of 30-40 min should continue.
- This study is the first district-specific approximation of how mesh size can affect various catch metrics by the fishery. Repeating this study in future years would provide data from runs that likely differ with respect to age-specific LFDs and the weight-length relationship (i.e., condition or plumpness, which affects the shape of the selectivity curve).
- In the interim, 4⅝" mesh is currently our best all-around prescription. While this recommendation many vary slightly as more data becomes available in the coming years, a firmer conclusion is that using meshes smaller than 5" (and definitely 5⅛") would increase the exploitation rate of 2-ocean fish while reducing that of 3-ocean fish.
- This outcome would benefit the fishery and management in several ways. Quantifying the extent to which these benefits would be realized will require additional work, but for now we can at least comment on the directions of how exploitation rates would change.
    - Switching to smaller gear should help prevent over-escapement of large 2-ocean runs to the Wood River.
    - Not only would smaller gear select 3-ocean fish less, but perhaps even more importantly a more efficient fleet would mean more closures. Both mechanisms would promote greater escapement of Nushagak River Sockeye as this stock tends to be dominated by 3-ocean fish.
    - More closures would also reduce exploitation of Chinook Salmon bound for the Nushagak River.

2020 Season

The purpose of the 2020 Nushagak District test fishery was similar to that for 2019. As such, the objectives and methods remained the same, but were adjusted based on recommendations learned from the 2019 data. Unlike 2019, only one net configuration was used based on the 2019 recommendation that the 150-fathom net comprised of six 25 fathom shackles alternating in mesh sizes (4½" and 5⅛") was optimum for our research purposes.

A total of 70 sets were made in the Nushagak District during June 16 to July 2 resulting in a total catch of 1,782 Sockeye (85% or 1,508 fish) were measured for length. Test fishing (sets using the TF protocol) occurred for eight days (June 16-June 24) prior to the first commercial fishing opener on June 25. Selection of station locations was again exploratory in nature, but more evenly distributed throughout the eastside of the District compared to 2019. Test fishing CPUE appeared to track the buildup of fish in the District prior to the first opener. The ratio of Sockeye:Chinook estimated from the test fishery catches off a bit in magnitude as compared to this ratio estimated for the reconstructed runs in the District. Nevertheless, spikes in this ratio from the test catches and the reconstructed runs seemed to align.

The 2020 selectivity curve was very similar to the 2019 curve, for which strong evidence against bias was provided. We applied the 4½" and 5⅛" mesh selectivity curves to the observed 2020 length frequency distribution (LFD) for the entire Nushagak District abundance to predict catch percentages for the meshes. We then compared these percentages to what was observed in both the TF and CF protocols. During openers when the CF protocol was used, we observed that 73% of the catch came from the 4½" mesh—nine percentage points greater than our prediction of 64%. During closures when the TF protocol was used, the observed percentage was closer (70%), but still six percentage points greater than the predicted 64%. The phenomenon of larger fish being filtered by the fishery would have to have occurred at a greater rate as compared to 2019 to completely explain the TF-CF catch percentage difference in 2020.

The observed size selectivity by the fishery appeared to be dome shaped and more consistent across a wider range of sizes than any particular individual mesh size. Across all fishermen, a range of mesh sizes was used which explains why this observed pattern occurred. Nevertheless, we approximated an average single mesh size used by the fishery (about 4⅝") while simultaneously adjusting the exploitation rate so that simulated catches for each age matched those observed. Then, holding this adjustment constant we changed mesh size from 4½" to 5⅛" by ⅛" increments and report the hypothetical performance of three objective functions: (1) maximize total catch, (2) maximize total lbs of catch, and (3) equalize exploitation rates across ages (Table 4).

The observed run was 63% 2-ocean and 37% 3-ocean sockeye. As predicted by the simulated run dominated by 2-ocean fish for the 2019 data (70% 2-ocean), the mesh size that maximized total catch, total lbs of catch, and equalized exploitation rates was estimated to be 4½". Furthermore, the 5⅛" mesh performed poorly in these regards, again as predicted by the 2019 simulated run of 70% 2-ocean fish.

Despite the predominant use of 5⅛" mesh size historically, there is reason to believe that fishermen are adapting. The 2018 Nushagak District run was the greatest on record (34 million) to which an above average exploitation rate was applied by the fleet. The following year (2019; 18 million), the exploitation rate was even greater and was spread more evenly across a broader range of sizes. Exploitation was lower for 2020 due to a smaller run size (13 million) but remained more evenly distributed across sizes. On explanation could be that a larger portion of the fleet is shifting to smaller mesh sizes. Due to the shape of the estimated selectivity curve, this occurrence would harvest more smaller fish without foregoing larger fish thereby flattening the selectivity curve for the fleet in general.

Recommendations for future work remain the same as those following the 2019 test fishery. We emphasize that the management implications from both years indicate mesh sizes ≤ 4¾" will more efficiently prevent over-escapement of age-1.2 Sockeye to the Wood River while not foregoing catch of age-1.3 Sockeye due to the shapes of the estimated selectivity curves in both years. A more efficient fleet will mean more closures to allow passage of age-1.3 Sockeye and Chinook Salmon to the Nushagak River.

Table of Contents

LIST OF TABLES

LIST OF FIGURES

INTRODUCTION

In 2019, a district test fishery was operated to assess the abundance, run timing, and size composition of the Sockeye return to the Nushagak commercial fishing district in Bristol Bay. The primary purpose of this endeavor was to provide daily information to the area management biologist (Tim Sands) regarding the buildup of fish in the district early in the season before they enter their natal river systems. In addition, length data from fish captured in the test net were used to characterize the size selectivity of gillnets across a range of mesh sizes.

Test fishing has been used in the Nushagak District in previous years to assess Sockeye abundance and guide when to open the commercial fishery. Oftentimes in the past, test fishing occurred upstream of the upper boundary of the commercial district to foretell escapement counts at enumeration sites in the Wood and Nushagak rivers. These years were characterized by managers working to ensure there were enough fish committed to moving into the rivers' escapement to allow a fishing period in the district. The purpose of the 2019 test fishery was focused on assessing the early, fishable abundance in the district to reduce the possibility of very a large passage of fish into the escapement early in the season. As such, the test fishery occurred where the commercial fishery takes place.

A secondary motivation for this project was to estimate contact selectivity curves for gillnets in the commercial fishery. Selectivity curves can be used to identify mesh sizes that will optimize the fleet's effectiveness at exploiting harvestable surpluses from the district's river-specific stocks. For example, gillnet mesh sizes may be selected to more effectively target smaller 2-ocean fish to prevent over escapement in a productive stock (e.g., Wood River) while protecting 3-ocean fish from a weaker stock (e.g., Nushagak River).

Net selectivity research over the last 10 years at the Port Moller Test Fishery (PMTF) has provided insight into what mesh sizes may be optimal in the inshore commercial fishing districts. However, fishing protocol, water clarity, and environmental conditions at Port Moller are different than in the inshore fishing districts. This project provided data to develop selectivity curves under the conditions and fishing methods the commercial fishery experienced in the Nushagak District.

As stated, the primary intent of this research was to detect fish aggregating in the district early in the season. However, the methods and results describing this endeavor are disproportionately shorter than those for the selectivity research simply owing to their relative complexities (even more detailed methods for estimation of the selectivity curves are provided in Appendix A). This report presents the results for both the 2019 and 2020 Nushagak District test fisheries. The main body describes the objectives, methods, and results for 2019. The objectives and methods remained unchanged for the 2020 test fishery; as such, we simply update the results for 2020 in Appendix B.

OBJECTIVES

1) Assess the daily abundance of Sockeye salmon in the Nushagak commercial fishing district using standardized test fishing methods;
2) Develop mesh-size-specific selectivity curves for two fishing protocols across a range of mesh sizes available to the commercial fleet by measuring all fish caught in the 4½" and 5⅛" panels of the test net. Separate sets of selectivity curves were estimated from two fishing protocols:

a. **<u>Standardized (PMTF) protocol</u>**: These were sets made during fishery closures whereby the test net was fished the same as the PMTF (the net was stretched to length during the set and no attempt was made to scare fish towards it);

b. **<u>Commercial Fishing Protocol</u>**: These were sets made during fishery openers with the net fished as it would be if it were being used in the commercial fishery (i.e., the net was hooked, and the boat "ran" the length of the set similar to commercial practice;

3) Based on the selectivity curve that best represents a fishing protocol used by a commercial fisherman, estimate mesh sizes that optimize total catch, total lbs of catch, and equalize escapement and total run age compositions (i.e., equalize exploitation rates across ages).

METHODS

The test fishery was conducted by the *F/V Seahawk* for 22 days beginning on June 15 and ending July 7. There were two fundamental components to the data collected from this test fishery:

1. **Test Fish Index**: The number of fish caught standardized to a unit of time (on hour) and total net length (200 fathoms) indexed fish buildup in the district, which helped to gauge run strength.
2. **Lengths of Fish in the two mesh sizes**: Fish length measurements binned by mesh size allowed estimation of contact selectivity curves for various mesh sizes and fishing protocols.

Below we provide the methods for collecting these data. Then, we describe the algorithm used for estimation of contact selectivity curves and how these curves were used to determine optimum mesh size for the Nushagak District in 2019.

Stations Fished

Locations fished were chosen by the skipper and the Area Management Biologist, Tim Sands. Their choice of stations was influenced by known primary migration routes, logistical limitations, weather, and the need to quantify the expanse of large schools of fish; stations were dropped or added as the season progressed. In addition to assessing the 2019 run, this year's effort was somewhat of a pilot study to inform how to design a district test fishery in future years; therefore, the locations of sampling stations were somewhat fluid. Station locations are depicted in Figure 1; coordinates for all stations are given in Table 1.

Net Configuration

Similar to the station selection, design of the test net configuration for 2019 was exploratory and changed throughout the season depending on catch rates, shifting objectives, and patchiness of the catches throughout the net. All test configurations were comprised of panels (shackles) alternating between two mesh sizes—either 4½" and 5⅛" meshes or 4½" and 4¾" meshes. Total net lengths, shackle lengths, mesh sizes, and the dates each configuration was used are given in Table 2. All net configurations were 29 meshes deep.

Fishing Protocols

<u>Deploying the Test Net</u>. —Retrieving the net took longer than deploying; therefore, it was best to switch which end of the net was in the water first and retrieved first at each subsequent set. Weather and tidal

conditions permitting, the net was set and retrieved so that the end of the net that was in the water first was the first end of the net retrieved. This provided approximately equal fishing time for each mesh over all the sets.

<u>During Closures</u>. —Fishing at each station consisted of one set using the standardized protocol (termed "TF" for test fishing) developed for the PMTF. For the TF protocol, the net was set in a linear fashion (no hook) and the vessel moved as far away as possible while maintaining visual contact.

<u>During Commercial Fishing</u>. —No stations or sampling protocols were assigned during open commercial fishing periods. The skipper actively engaged in the commercial fishery and had full discretion to fish when, where, and how he chose. However, the general idea was that the net was fished as it would be during a commercial opener to try and maximize catch.

Based on gillnet selectivity research at the PMTF, we estimated that a mesh size of 4¾" would optimize commercial catch efficiency (i.e., the number of fish caught) for an average year. To test this hypothesis, we replaced the 5⅛" panels with 4¾" panels (while keeping the alternating 4½" panels) and fished this net instead for four consecutive days during the commercial fishery (Table 2).

Data Collection

<u>Fish Counts by Mesh</u>. —During retrieval, the entire catch was removed from the gillnet and placed in mesh-specific totes. Each Sockeye was measured for length (mid-eye fork length, MEFL) and the number within each cm length bin was recorded by mesh size. Other species of salmon were counted, but not sampled further. The length sampling goal for Sockeye was 100% of the entire set's catch; subsampling lengths from a given set was of no value with respect to selectivity estimation. However, during a few high catch sets (three in total) lengths were not recorded because not all Sockeye could be measured.

<u>Net Length and Mean Fishing Time</u>. —As area manager needed station- and date-specific catch indexes of abundance each set had to be standardized to a common net length and fishing time; i.e., catch-per-unit-effort (CPUE). Thus, all catches were standardized to how many fish would have been caught from fishing a 200-fathom net for one hour. First, catch was divided by the total length of the net measured in fathoms and then multiplied by 200. Second, this adjusted catch was divided the mean fishing time (MFT) measured in minutes, then multiplied by 60. Because the net begins fishing before it has been fully deployed and fishes while being retrieved, this time must be accounted for in addition to the time the net is fully deployed. Mean fishing time was calculated as follows:

$$\mathrm{MFT} = [\mathrm{C} - \mathrm{B}] + \frac{[(\mathrm{B}-\mathrm{A})+(\mathrm{D}-\mathrm{C})]}{2} \qquad (1)$$

Where A = the time net deployment began, B = the time net deployment ended, C = the time net retrieval began, and D = the time net retrieval was complete.

<u>Environmental Data</u>. —Environmental conditions, such as water characteristics, weather conditions, and tide stage may affect the vulnerability of fish and the efficiency of capture gear. Also, environmental factors are important determinants of annual run timing and patterns. Thus, such data were collected during each gillnet deployment to identify possible correlations between environmental factors and the test fishery catch. While no correlations have been statistically estimated to date, the following variables were recorded and are available for future analyses:

- **Lat/Long:** Latitude/longitude of each set, in decimal degrees.

- **Wind Direction**: This condition was typically obtained from wheelhouse instrumentation and was recorded to the nearest 8-point cardinal compass bearing (N, NE, E, etc.).
- **Wind Velocity** (knots): This condition was approximated.
- **Tidal Stage:** High slack, ebb, low slack, or flood.

Selectivity Curve Estimation and Verification

Separate contact selectivity curves were developed for (1) the TF protocol using the 4½" and 5⅛" mesh configuration, (2) the CF protocol using the 4½" and 5⅛" mesh configuration, and (3) the CF protocol using the 4½" and 4¾" mesh configuration. Separate curves were also estimated from two datasets generated by the 2019 PMFT—one from the R/V *Pandalus* and one for the F/V *Ocean Cat*.

Detailed statistical methods for curve estimation is provided in Appendix A. Briefly, the selectivity curves were estimated indirectly by adjusting the number of fish in each cm size bin caught from both paired meshes in a given dataset until the shape of the selectivity curve was revealed (see Figure A1 in Appendix A) as per Tang et al. (2010). Unlike other algorithms (e.g., Millar 1992), this method requires no assumption regarding the shape of the selectivity curve.

Two approaches were used to verify that the general shape of the estimated curves was unbiased. First, using methods described in Appendix A, we superimposed the estimated CF-4½" and 5⅛" mesh curve onto a typical oceanic phase Sockeye to illustrate how selectivity changed along likely capture points. Second, we compared expected catches between the 4½" and larger meshes based on the estimated selectivity curves to what was observed. Assuming the test fishery was exposed to a sample of ages/sizes representative of the entire run, then observed and expected catches should match.

RESULTS AND DISCUSSION

A total of 92 sets were made in the Nushagak District during June 15 to July 7 resulting in a total catch of 6,680 Sockeye (49% or 3,283 fish were measured for length; Table 2). Three different configurations for nets comprised of 4½" and 5⅛" meshes were used varying in total net length and individual shackle length. An additional configuration was used during the middle of the commercial fishery whereby the 5⅛" mesh was replaced with 4¾" mesh. According to our technician, the 150-fathom net with 25 fathom shackles was optimum for our research purposes (Munroe Morris, pers. comm., July 8, 2019). That is, a 150-fathom net was manageable during repetitive high catch sets and afforded greater opportunity for the collection of fish lengths (unlike the 200-fathom net). Furthermore, the more frequent mesh size change with alternating 25 versus 50 fathom shackles increased the randomness of each mesh size's encounter to dense schools of fish (unlike the 100-fathom net with two 50 fathom shackles). As a result, six 25 fathom shackles alternating in mesh size should help reduce noise in the selectivity data.

Test Fishing to Detect Fish Abundance in the Nushagak District

Test fishing (sets using the TF protocol) occurred for six days (June 15-June 20) prior to the first commercial fishing opener on June 20; one TF protocol set happened on June 21 after an opener had closed on that date and another occurred on July 7 to acquire data from this protocol using the 150-fathom net with 25-fathom shackles net configuration (Table 2). Despite the exploratory nature of selecting station locations (Figure 1), test fishing CPUE did appear to track the buildup of fish in the district during June 15-June 21 (Figure 2A). Likewise, the daily estimates of the Sockeye:Chinook ratio in the test catches seemed to follow that estimated for the reconstructed runs in the District (Figure 2B).

Standardizing the net configuration and stations fished in future years should improve this correlation. As mentioned, using a 150-fathom net with 25-fathom shackles of alternating mesh worked well. The stations fished varied a bit, but most were located west/southwest of Ekuk, Alaska. Finally, while no specific instructions were given to the crew regarding target mean fishing times (MFTs), they appear to have tried for 30-40 min, which got extended when catches were high (Figure 3). Mean fishing times averaged 40 min (range=31-55 min), but as expected greater catches took longer to pick and subsequently increased MFTs. Nevertheless, higher MFTs were accounted for when catch was converted CPUE, and a 30-40 min MFT target in the future seems reasonable.

Once commercial fishing commenced on June 21 and the commercial catch was strong (similar to the previous two years), test fishing data was likely of marginal utility to the manager. After this date, high commercial fishing effort (overall exploitation rate=0.83) was used to prevent/minimize over-escapement into the three systems from a total Nushagak District run of 17.8 million Sockeye.

Typically, the manager tries to spread escapement across the entirety of the season in proportion to the run, all the while guarding against over- or under-escaping. Seasons 2019 and 2018 are good examples of years when escapement was not overly front loaded at the beginning and was spread proportionately throughout the season (Figure 4). However, early runs (2+ days) such as 2003, 2011, and 2013 or very small runs, e.g. 2012, can cause a disproportionate total of the escapement to occur before commercial fishing begins. For instance, in 2013 40% of the escapement had occurred by June 22 compared to only 4% of the catch through that date (Figure 5). During these types of years, a standardized test fishery could facilitate the manager's decision to initiate fishing effort earlier than usual; this scenario assumes of course there is enough fishing power in the District to impose a nontrivial exploitation rate.

Selectivity Curves for the Nushagak District

Throughout the season, three net configurations, two different mesh pairings, and two fishing protocols were tested resulting in seven datasets (not all combinations were tried; see Table 2). For selectivity curve estimation, we chose to use only the dataset from the 150-fathom net length/25-fathom shackle combination for the CF protocol with 4½" and 5⅛" meshes. We reasoned that this dataset provided the least biased estimation of the selectivity curve shape under commercial fishing conditions because fish were more randomly exposed to each mesh, and the sample size was large (n=1,299). However, both 100- and 150-fathom net length configurations were used for the TF protocol as sample sizes were limited (n=621 and 266, respectively [total=887]); only one configuration was available for the CF protocol with 4½" and 4¾" meshes (n=529).

Estimated selectivity curves for 4½" and 5⅛" meshes under the CF protocol are shown in Figure 6. Peak selectivity for the 4½" mesh occurred across the size range for ocean-age 2 fish while that for the 5⅛" mesh occurred over ocean-age 3 fish lengths. However, the relative selectivity differentials are not the same; that is, the 4½" mesh is more selective for ocean-age 3 fish than the 5⅛" mesh is for ocean-age 2 fish. This finding has important ramifications for estimating mesh sizes that optimize catch efficiency. Below we first examine and offer potential reasons for the differences among selectivity curves developed for the Nushagak District Test Fishery versus those for 2019 PMTF. Then, we investigate the potential for bias in the CF 4½"-5⅛" selectivity curve. Both endeavors were necessary if we are to have confidence in using this curve to recommend mesh sizes to optimize efficiency in the commercial fishery.

<u>*Comparison of Selectivity Curve Shapes*</u>. —As mentioned in the methods detailed in Appendix A, fish lengths had to be divided by mesh circumference (l_j/m_i) to allow for indirect curve estimation. This exercise also facilitates comparison of varying curve shapes across protocols independent of mesh size (Figure 7). In all, three different curves were generated from the Nushagak test fishing data and appeared to be more or less similar with some exceptions. Given that the net configurations used to generate the TF and CF 4½"-4¾" mesh curves were prone to more uncertainty and bias due to lower sample sizes and less random fish exposure to the mesh sizes, we will refrain from attempting to assign causation to these exceptions. For now, it is simply worth noting that they were similar to the CF 4½"-5⅛" curve. Two additional curves were generated from the PMTF, which differed slightly from each other and more substantially from the Nushagak curves.

Any real differences among curves could have been caused by several reasons including variations in: (1) girths at given lengths, (2) fish behavior, (3) fishing protocols, and (4) dropout rates during net picking. Before explaining these possibilities, we first note that there appears to be three modes corresponding to the three capture mechanisms identified by Baranov (1914). As shown below under the *Curve Verification* section, from right to left these modes correspond to fish being tangled, gilled, and wedged (Figure 8). Konda (1966) identifies seven capture mechanisms. However, in all practicality these mechanisms reduce to the three identified by Baranov (1914); furthermore, he considered the tangled mode to be insignificant.

Fusiform, smooth bodied fish, such as Sockeye, are mostly wedged (Taguchi 1961; Konda 1966). Of the three, the location and height of the wedged mode (and the left side of the curve in general) is affected more than the others by the reasons listed above. However, because it is the highest mode and curves are scaled to a maximum height of one, variability among curves vertically along the y-axis often appear more pronounced towards the right side of the curve over the gilled and tangled modes, which is misleading. Inspection of Figure 7 demonstrates this artifact across the curves generated for this study (Note: sample sizes were too low for the tangle mode to be estimated for the Nushagak TF and CF 4½"-4¾" mesh curves).

Ishida (1967) says the left side of the curve is more affected (lowered) by small decreases in relative girth; large decreases in relative girth can shift the entire curve right along the x-axis. Hamley (1975) also notes that curves are narrower and normal shaped when fish are mostly wedged but tend to be broader and skewed right as more fish become gilled and tangled. The wedged modes for the Nushagak curves were shifted right versus those for Port Moller. This result could have been caused by differences in relative girths among the fish exposed to each test fishery; i.e., Port Moller was exposed to fatter fish on average. It is worth noting that the Nushagak curves are more similar to the curve developed from the F/V Ocean Cat, which mostly fished the outer stations at Port Moller where Nushagak fish are prone to migrate. The R/V Pandalus fished mostly inside stations and would have been more exposed to Egegik and Ugashik fish.

Other differences may have been caused by fish hitting the net harder in the Nushagak test fishery and thereby increasing the depth of capture along the body. Water clarity is drastically diminished in the Nushagak District versus the Port Moller transect making the net more difficult to detect. Furthermore, fishermen run back and forth during sets in an attempt to drive more fish into the net. Both of these factors may have increased the average swimming speed at which fish contacted the net. If fish in the Nushagak test fishery pushed deeper into the net, then one would expect a higher gilled and lower tangled mode as was observed compared to Port Moller curves.

Finally, dropout rates may have been higher in the Nushagak District versus Port Moller. According to our technician, dropouts occurred more readily for fish caught deep in the body close to the dorsal fin insertion than compared to those that were tangled. Fish pushing deeper into the net because of increased swimming speeds would increase this occurrence; the result would be to skew the selectivity curves right.

Curve Verification. —The algorithm used in this study required no assumptions regarding the shape of the selectivity curves (Tang et al 2010). The resulting patterns consistently showed modes in distinct locations along the l_j/m_i axis. We converted the l_j/m_i values to depths of capture and expressed them as proportions of fork length using Equation A5 (Appendix A). This exercise allowed for a selectivity curve to be superimposed onto an illustration of a typical oceanic phase Sockeye (Figure 8) and facilitated understanding of where the respective modes occurred in relation to the fish's anatomical features. The tangle mode appears to have occurred posterior to the pre-operculum, the gilled mode just behind the gill cover, and the wedged mode further toward the dorsal insertion. This finding agrees with observations of where along the body fish are mostly likely to be caught and suggest that the location and relative heights of these modes as estimated with the indirect contact selectivity curves were reasonable.

We developed curves for 4½", 4¾", and 5⅛" meshes and applied them to the observed length frequency distribution (LFD) for the entire Nushagak District abundance to predict catch percentages between the 4½" mesh and the larger meshes. We then compared these percentages to what was observed when we fished the various mesh pairings (Table 3). During openers when the 4½"-5⅛" mesh pairing and CF protocol was used, we observed that 65% of the catch came from the 4½" mesh—five percentage points greater than our prediction of 60%. Likewise, the observed 4½" catch percentage of 56% for the 4½"-4¾" pairing was five percentage points greater than our prediction of 51%, which also occurred during openers. In other words, we underpredicted the advantage that the 4½" mesh would have over two different larger meshes by a consistent amount during openers. One explanation could be that our predictions were based on the LFD for the entire run and not representative of the LFD that existed in the District during openers when larger fish were likely filtered by the commercial fishery, thereby giving the 4½" mesh an even larger advantage. One would expect then that the observed 4½" catch percentage during closures, when the run was unfiltered by the fishery, would be closer to our prediction. The observed percentage of 59% was closer to the prediction of 60% during closures when the TF protocol and 4½"-5⅛" pairing was used.

Comparing observed and expected catch LFDs for the CF protocol and 4½"-5⅛" mesh combination (150 fathom net with alternating 25 fathom shackles) to the age-specific abundance LFDs illustrates this point further (Figure 9). These test net samples were spread throughout the season (Figure 2). On these dates (June 20-24 and June 30-July 7) the middle 50% of C+E occurred, thus increasing the chances that samples were exposed to a representative LFD of the run. Front- or back-loaded samples may have encountered a passing LFD that was not indicative of the entire District's run. Such a scenario would still generate unbiased indirect "contact" selectivity curves (see Appendix A for definition of contact selectivity) but would cause observed and expected catch LFDs to differ. However, as noted above samples collected during a commercial opener may be biased towards smaller sized fish due to the commercial fishery targeting larger sized fish. In Figure 9, we see that the observed and expected catch LFDs for both meshes line up reasonably well. Observed catches were slightly greater than expected over the 47-49 cm bins for the 4½" mesh, which represent the most abundant sizes for age-1.2 Sockeye. Catches were lesser than expected over the 52 and 53 cm bins for both meshes, which were closer to the peak abundance for age-1.3 Sockeye.

Finally, the even age composition for the Nushagak District run (52% OA2 and 48% OA3) caused the relative heights of the catch LFDs to be similar. If fish in the cm bins most selected for by a given mesh contact the net more than those in bins most selected for by another mesh, then catch curve heights will differ between meshes. Again, the difference in mesh heights for the observed catches is understandable if the commercial fishery caused larger fish to be filtered from the run before it reached the test fishing net. In summary, the illustrated catch mechanics suggest that the contact selectivity curves were unbiased.

Optimizing Selectivity Curves for the Nushagak District

Once the shape of the selectivity curve along the l_j/m_i axis was estimated based on the CF 4½”-5⅛” dataset, a curve for any mesh size could be approximated (i.e., in addition to the two meshes used to estimate the curve). The observed size selectivity by the fishery appeared to be dome shaped and more consistent across a wider range of sizes than any particular individual mesh size (Figure 10). Across all fishermen, a range of mesh sizes was used which explains why this observed pattern occurred; anecdotal conversations with various fishermen indicate that during 2019, mesh sizes ranged at least from 4½” to 5⅛”. Nevertheless, we approximated an average single mesh size used by the fishery (about 4⅝”) while simultaneously adjusting the exploitation rate so that simulated catches for each age matched those observed. Then, holding this adjustment constant we changed mesh size from 4½” to 5⅛” by ⅛” increments and report the hypothetical performance of three objective functions: (1) maximize total catch, (2) maximize total lbs of catch, and (3) equalize exploitation rates across ages (Table 4). In addition, two simulated runs comprised of 70% 3-ocean and 30% 3-ocean fish were created, and mesh sizes were re-estimated for the same objective functions. The same LFDs for each age were assumed for each simulated run.

The observed run was about evenly split between 3-ocean (48%) and 2-ocean (52%) fish. The mesh size that maximized total catch and equalized exploitation rates was estimated to be 4½”, while 4⅝” mesh was estimated to maximize total lbs of catch (Table 4). Had the run been 70% 3-ocean fish, slightly larger meshes would have been more effective to maximize total catch (4¾” mesh) and total lbs (4⅞” mesh). A 30% 3-ocean run would have had all three objective functions optimized with 4½” mesh. Because identical age-specific LFDs were assumed for the observed and simulated runs, it makes sense that 4½” mesh was estimated to equalize exploitation rates across ages for all three scenarios.

Some additional results are noteworthy. First, 4⅝” mesh performed well even when the run’s age composition was shifted towards and away from 3-ocean fish (i.e., 70% and 30% 3-ocean runs, respectively). That is, exploitation was more even between the two ocean ages without giving up too much efficiency in maximizing total lbs of catch. The consequence of this finding is that potential evolutionary changes incurred from artificial selection by the fishery could be removed without loss of profits. Though the evolutionary influence of gillnet fisheries on Sockeye have been judged nominal (Todd and Larkin 1971), Kendall and Quinn (2007) considered there to be potential for this occurrence in the Bristol Bay fishery.

Secondly, 5⅛” mesh performed poorly in these regards even when the age composition was shifted towards 3-ocean fish. Catch efficiency for the 5⅛” mesh was the lowest across the range of meshes for all scenarios. This mesh size was the predominant mesh used historically and has lingered in the fishery perhaps as a carryover from the regulations and/or processors encouraging this larger mesh to increase average individual sizes in the catch for when processing capacity was more limiting. Kendall et al. (2009) summarized the history of the gear used in Bristol Bay. Regulations allowed for a minimum of 5¾” mesh to be fished from 1924 to 1961. In 1962, the minimum was further reduced to 5⅜” to reduce pressure on larger fish. It was thought that these mesh sizes caught disproportionately more males than females, and therefore, increased spawning success of the escapement. After 1984, the minimum mesh size regulation was lifted (Helton 1991). A journal kept by the most common supplier of gillnets to Bristol Bay fishermen documents that the most common mesh size ordered over the previous 25 years was 5⅛” (T. Reed, pers. comm., Seattle Marine and Fishing Supply Co., 2011).

Our results indicate that greater catches can be achieved with mesh sizes smaller than conventional wisdom would lead us to believe. Of course, the overall seasonal catch would not increase from optimizing mesh sizes because specific openings/closures are determined based on escapement counts. Rather, the total time for openings would be reduced to counter this increased efficiency in the fishery.

FUTURE WORK RECOMMENDATIONS AND MANAGEMENT IMPLICATIONS OF THE SELECTIVITY RESULTS

The value of the 2019 Nushagak test fishery for improving management efficiency was marginal as the run was large and more-or-less-continued openers began early in the season. This utility should increase in years with early and/or small runs. Standardizing the net configuration and stations fished in future years should improve the correlation between test fishing CPUE and fish buildup in the District. A 150-fathom net with 25-fathom shackles of alternating mesh worked well to better randomize exposure of individual schools of fish to each mesh size. Continued exploration of station locations should continue for at least one more year before fixed station sites are established. Finally, target mean fishing times of 30-40 min should continue.

This study is the first district-specific approximation of how changing mesh size can affect various catch metrics by the fishery. Repeating this study in future years would provide data from runs that likely differ with respect to age-specific LFDs and the weight-length relationship (i.e., condition or plumpness, which affects the shape of the selectivity curve). In the interim, 4⅝” mesh is currently our best all-around prescription. While this recommendation many vary slightly as more data becomes available in the coming years, a firmer conclusion is that using meshes smaller than 5⅛” would increase the exploitation rate of 2-ocean fish while reducing that of 3-ocean fish. This outcome would benefit the fishery and management in several ways. Switching to smaller gear should help prevent over-escapement of large 2-ocean runs to the Wood River. Not only would smaller gear select 3-ocean fish less, but perhaps even more importantly a more efficient fleet would mean more closures. Both mechanisms would promote greater escapement of Nushagak River Sockeye as this stock tends to be dominated by 3-ocean fish. More closures would also reduce exploitation of Chinook Salmon bound for the Nushagak River. Quantifying the extent to which these benefits would be realized will require additional work, but for now we can at least comment on the directions of how exploitation rates would change.

ACKNOWLEDGEMENTS

To be completed.

REFERENCES

Baranov F. I. 1914. The capture of fish by gillnets. Mater. Poznsniyu. Russ. Rybolovsta. 3:56–99. (Translation from Russian in 1976: Selected Works on Fishing Gear. Vol. I. Commercial fishing techniques. Israel Programme for Scientific Translations, Jerusalem.)

Hamly J M. 1975. Review of gill-net selectivity. *Journal of the Fisheries Research Board of Canada* 32:1943-1969.

Helton, D. 1991. An analysis of the Port Moller offshore test fishing forecast of Sockeye and chum salmon runs to Bristol Bay, Alaska. M.S. Thesis, University of Washington, Seattle. Thesis No. 38816.

Ishida, T. 1967. The salmon gillnet mesh selectivity curve. International North Pacific Fisheries Commission. Bulletin No. 26.

Kendall, N. W. and T. P. Quinn. 2009. Effects of population-specific variation in age and length on fishery selection and exploitation rates of Sockeye salmon (*Oncorhynchus nerka*). Canadian Journal of Fisheries and Aquatic Sciences 66:896-908.

Kendall, N. W., J. J. Hard, and T. P. Quinn. 2009. Quantifying six decades of fishery selection for size and age at maturity in Sockeye salmon. *Evolutionary Applications* 2:523–536.

Konda, M. 1966. Studies on the optimum mesh of salmon gill net. *Memoirs of the Faculty of Fisheries Hokkaido University* 14:1-88.

Millar, R. B. 1992. Estimating the size-selectivity of fishing gear by conditioning on the total catch. *Journal of the American Statistical Association* 87:962-968.

Millar, R. B. and R. J. Fryer. 1999. Estimating the size-selection curves of towed gears, traps, nets and hooks. *Reviews in Fish Biology and Fisheries* 9:89-116.

Taguchi, K. 1961. On the suitable mesh size on salmon gillnets inferred from the relationship between body weight of salmon caught by gillnets and its mesh size. *Bulletin of Japanese Society for the Science of Fish* 27:645-649.

Tang, Y., L. Huang, C. Ge, Z. Liang, and P. Sun. 2010. A new algorithm for estimating gillnet selectivity. Chinese Journal of Oceanology and Limnology 28:274–279.

Todd, I. and P. A. Larkin 1971. Gillnet selectivity on Sockeye (Oncorhynchus nerka) and pink salmon (O. gorbuscha) of the Skeena River system, British Columbia. *Journal of the Fisheries Research Board of Canada* 28:821-842.

Table 1. Coordinates and station designations fished during the 2019 Nushagak Test Fishery sorted by greatest to least catch-per-unit-effort (CPUE= number of Sockeye caught if a 200-fathom net had been fished for one hour). Note: these stations encompass all net configurations and fishing protocols (see Table 2).

Station	Substation	Longitude	Latitude	CPUE
41	SE41	158.3649	58.7038	510
24	SE24	158.6545	58.8289	338
24	S24	158.6547	58.8475	302
44	W44	158.6223	58.6576	296
32	S32	158.4913	58.7112	276
21	S21	158.6074	58.8008	266
33	N33	158.6177	58.7674	250
32	N32	158.5455	58.7702	205
34	S34	158.5636	58.7039	205
31	S31	158.4252	58.7216	188
32	SE32	158.4871	58.7270	176
32	W32	158.5266	58.7158	169
31	E31	158.3888	58.7307	158
41	N41	158.4435	58.7120	157
34	SW34	158.6246	58.6775	149
33	SE33	158.5769	58.7148	142
24	E24	158.6122	58.8425	131
21		158.5815	58.8014	129
33	NE33	158.5907	58.7692	128
32	NE32	158.4923	58.7518	110
43	N43	158.5508	58.6864	108
42	NE42	158.4608	58.7111	103
21	SE21	158.5763	58.8046	99
35	SE35	158.6597	58.6708	93
43	NE43	158.5096	58.6934	92
34	NW34	158.6680	58.7596	90
33	S33	158.6110	58.7314	75
21	SW21	158.6203	58.8048	74
31	N31	158.4698	58.7713	72
33	NW33	158.6263	58.7540	67
32	NW32	158.5551	58.7634	58
33	E33	158.5468	58.7179	56
32		158.5486	58.7750	51
43		158.5658	58.7299	49
33	SW33	158.5796	58.7225	44
21	W21	158.6327	58.8373	43
24	NW24	158.6096	58.8959	42
42	NW42	158.5100	58.6940	37
41	NW41	158.4406	58.6737	35
35		158.6587	58.7607	32
45		158.6506	58.6994	31
33		158.6139	58.7630	28
46	SW46	158.7725	58.5865	27
36	W36	158.7856	58.6050	22
44	NW44	158.6212	58.7163	21
54		158.5246	58.6166	12
34		158.6388	58.7746	7
35	SW35	158.6964	58.6292	5
24	W24	158.6465	58.8910	0

Table 2. Overview of the net configurations and fishing protocols by dates used in the 2019 Nushagak District Test Fishery. Protocol TF and CF stand for "test fishing" and "commercial fishing", respectively. All nets consisted of 4½" meshed shackles of varying lengths alternating with either 5⅛" or 4¾" meshed shackles.

Dates	Net length (fathoms)	Shackle length (fathoms)	Protocol	Mesh sizes (inches)	Number of sets	Sockeye catch	Lengths measured	% measured for length
Jun 15 - Jun 20	100	50	TF	4½-5⅛	28	694	621	89%
Jun 20 - Jun 21	200	50	TF	4½-5⅛	2	492	0	0%
Jun 20 - Jun 21	200	50	CF	4½-5⅛	2	75	75	100%
Jun 22 - Jun 24	100	50	CF	4½-5⅛	11	776	493	64%
Jun 26 - Jun 29	100	50	CF	**4½-4¾**	16	1,476	529	36%
Jun 30 - Jul 7	150	25	CF	4½-5⅛	32	2,901	1,299	45%
Jul 7	150	25	TF	4½-5⅛	1	266	266	100%
				Total=	92	6,680	3,283	Mean=49%

Table 3. Observed and predicted (from the selectivity curves) catch percentages between various mesh pairings used in the 2019 test fishing nets for the Nushagak District.

<table>
<tr><th>Protocol</th><th>Meshes fished (inches)</th><th>Obs. % of catch from 4½" mesh</th><th>Pred. % of catch from 4½" mesh</th></tr>
<tr><td>CF</td><td>4 1/2-4 3/4</td><td>56%</td><td>51%</td></tr>
<tr><td>CF</td><td>4 1/2-5 1/8</td><td>65%</td><td rowspan="2">60%</td></tr>
<tr><td>TF</td><td>4 1/2-5 1/8</td><td>59%</td></tr>
</table>

Table 4. Estimated catch metrics across various mesh sizes and run scenarios from the selectivity curve based on the CF 4½"-5⅛" dataset collected in the Nushagak District during 2019. Shaded values indicate optimized values.

Mesh size (inches)	Catch (individuals)	Fish wt. (lbs)	Catch (lbs)	Exploitation rate		Efficiency relative to mesh that max. lbs
				Age 1.2	Age 1.3	
Observed run with 48% ocean age 3 fish						
4 1/2	14,914,524	4.76	71,062,569	0.87	0.80	0.98
4 5/8	14,814,601	4.92	72,839,348	0.78	0.89	1.00
4 3/4	14,244,034	5.07	72,272,333	0.66	0.95	0.99
4 7/8	13,285,210	5.23	69,441,913	0.52	0.98	0.95
5	11,790,545	5.38	63,387,843	0.39	0.95	0.87
5 1/8	10,152,186	5.52	56,088,330	0.27	0.88	0.77
Hypothetical run with 70% ocean age 3 fish						
4 1/2	14,625,818	5.07	74,082,687	0.87	0.80	0.90
4 5/8	15,240,829	5.20	79,264,378	0.78	0.89	0.97
4 3/4	15,381,642	5.33	82,032,203	0.66	0.95	1.00
4 7/8	15,048,385	5.45	82,083,868	0.52	0.98	1.00
5	13,963,935	5.57	77,779,937	0.39	0.95	0.95
5 1/8	12,502,188	5.69	71,099,999	0.27	0.88	0.87
Hypothetical run with 30% ocean age 3 fish						
4 1/2	15,157,160	4.52	68,524,392	0.87	0.80	1.00
4 5/8	14,456,390	4.67	67,439,607	0.78	0.89	0.98
4 3/4	13,287,963	4.82	64,069,916	0.66	0.95	0.93
4 7/8	11,803,397	4.98	58,817,327	0.52	0.98	0.86
5	9,963,979	5.15	51,292,400	0.39	0.95	0.75
5 1/8	8,177,192	5.32	43,472,183	0.27	0.88	0.63

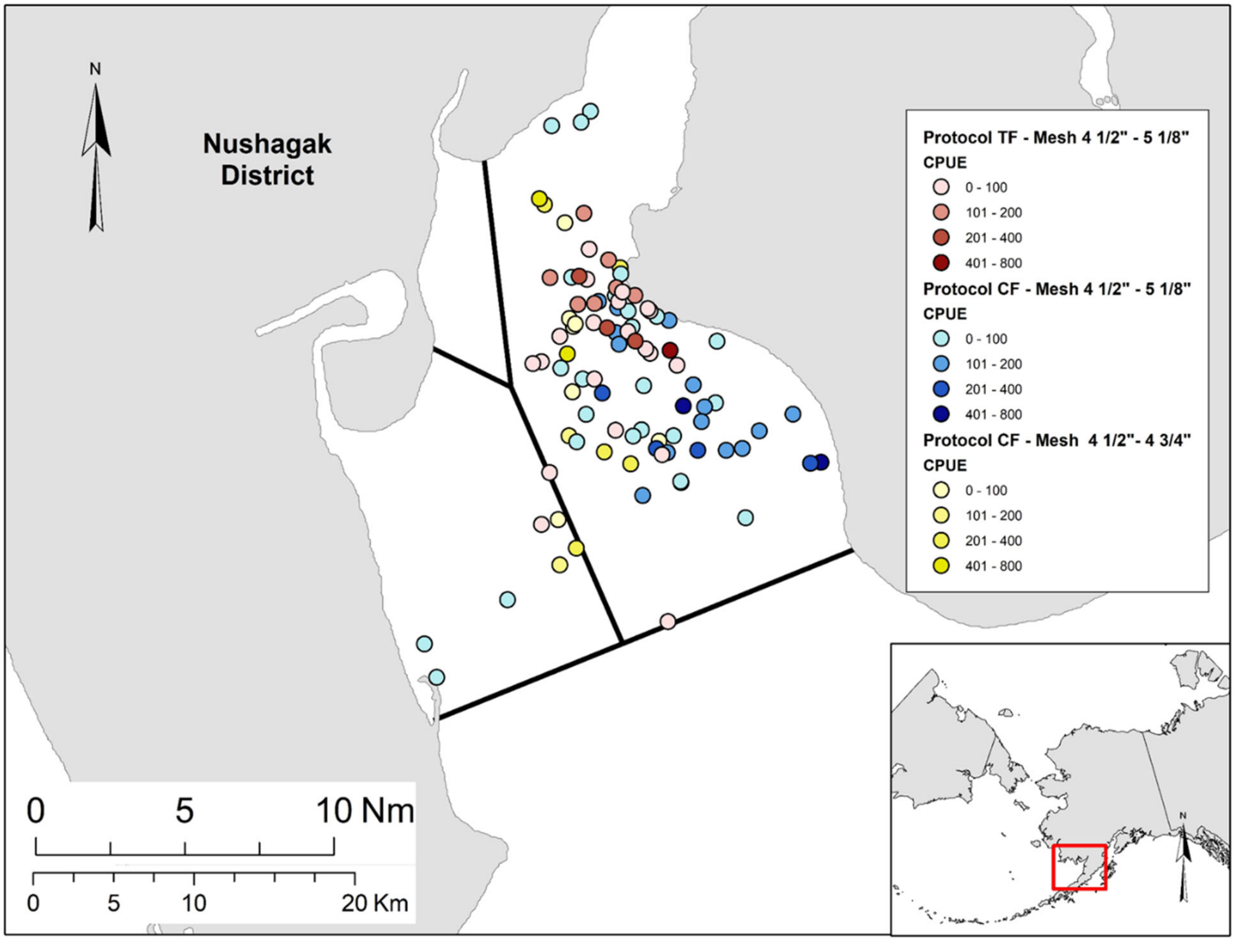

Figure 1. Location of stations fished during each fishing protocol/mesh size configuration combination. Intensity of color reflects greater catch-per-unit-effort (CPUE=number of Sockeye caught if a 200-fathom net had been fished for one hour).

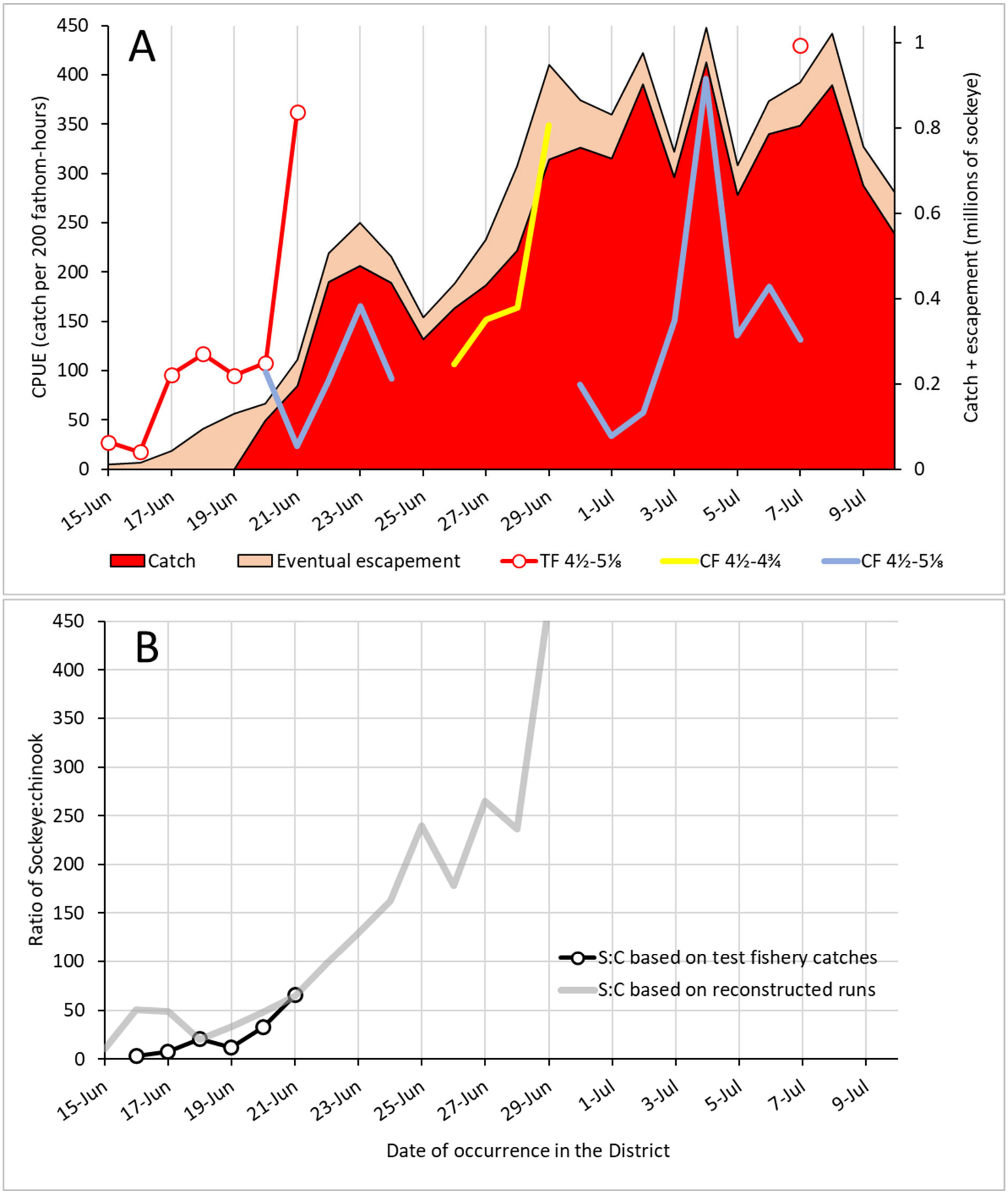

Figure 2. Test fishing indices. (A) CPUE (left y-axis) and catch + escapement (right y-axis) in the Nushagak District during 2019. Fishing by the test boat during closures is indicated by "TF" and "CF" during openers. The X-axis represents the date of occurrence in the district; thus, the escapement values depicted were combined from all three systems (Wood, Nushagak, and Igushik), each lagged back to the district by a number of days that varied across systems. (B) The ratio of Sockeye:Chinook in the TF catches versus that for the reconstructed runs.

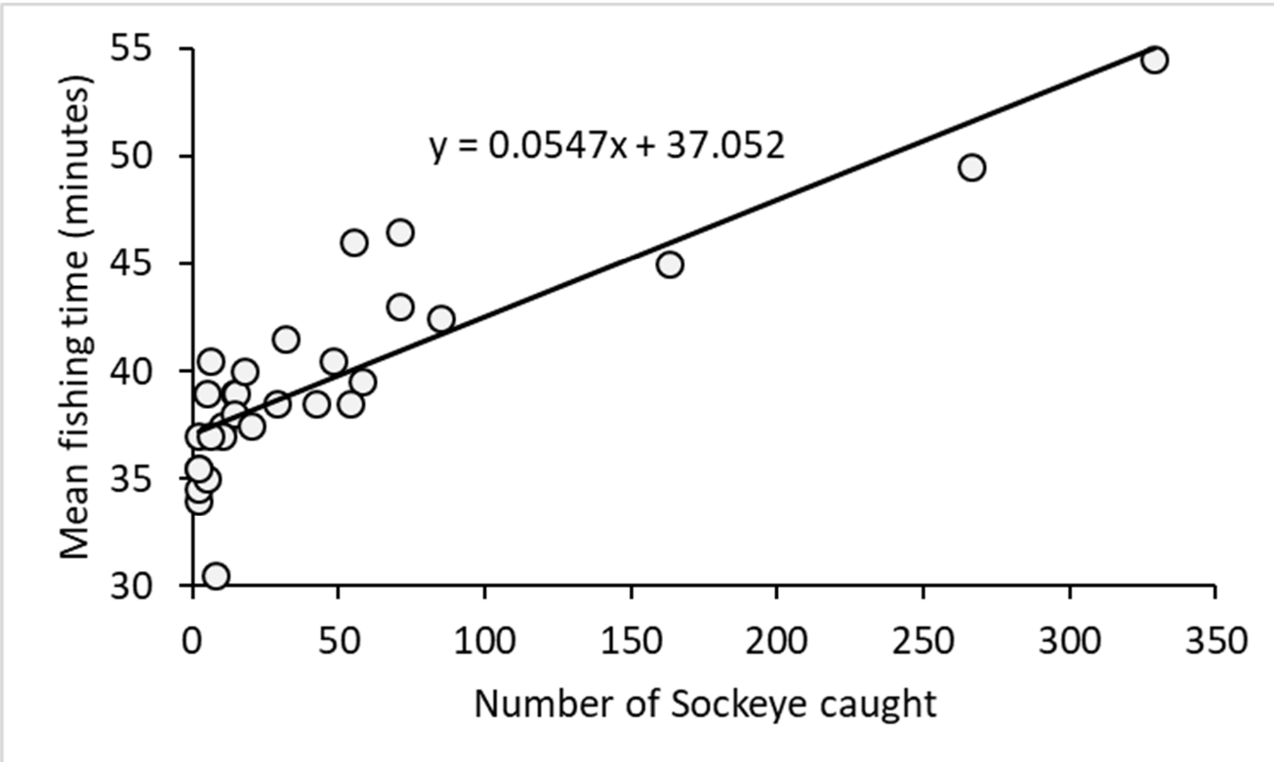

Figure 3. Mean fishing time versus total catch during the test fishing protocol (TF).

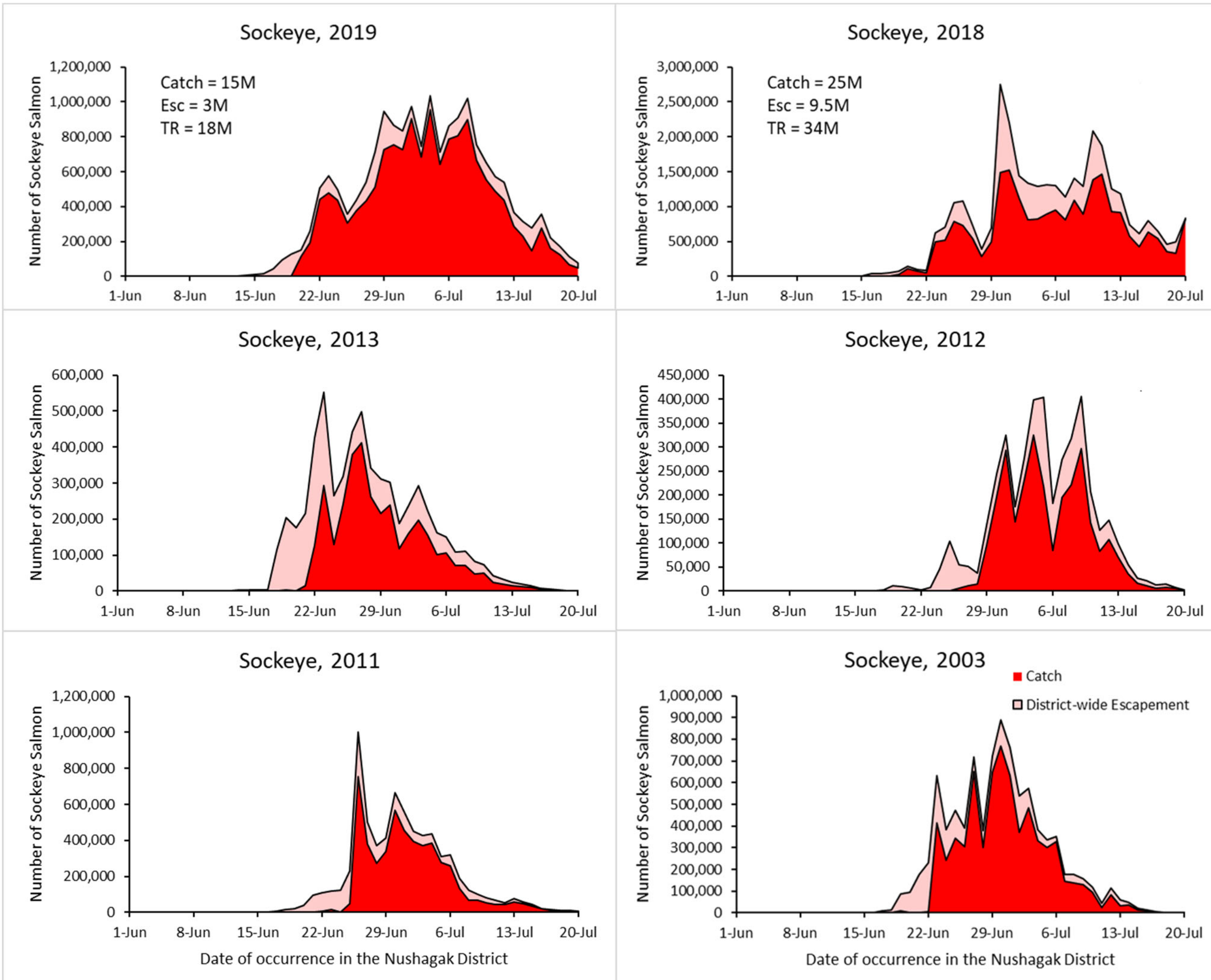

Figure 4. Catch + escapement across the entire season in the Nushagak District for various years. The X axis represents the date of occurrence in the district; thus, the escapement values depicted were combined from all three systems (Wood, Nushagak, and Igushik), each lagged back to the district by a number of days that varied across years and systems.

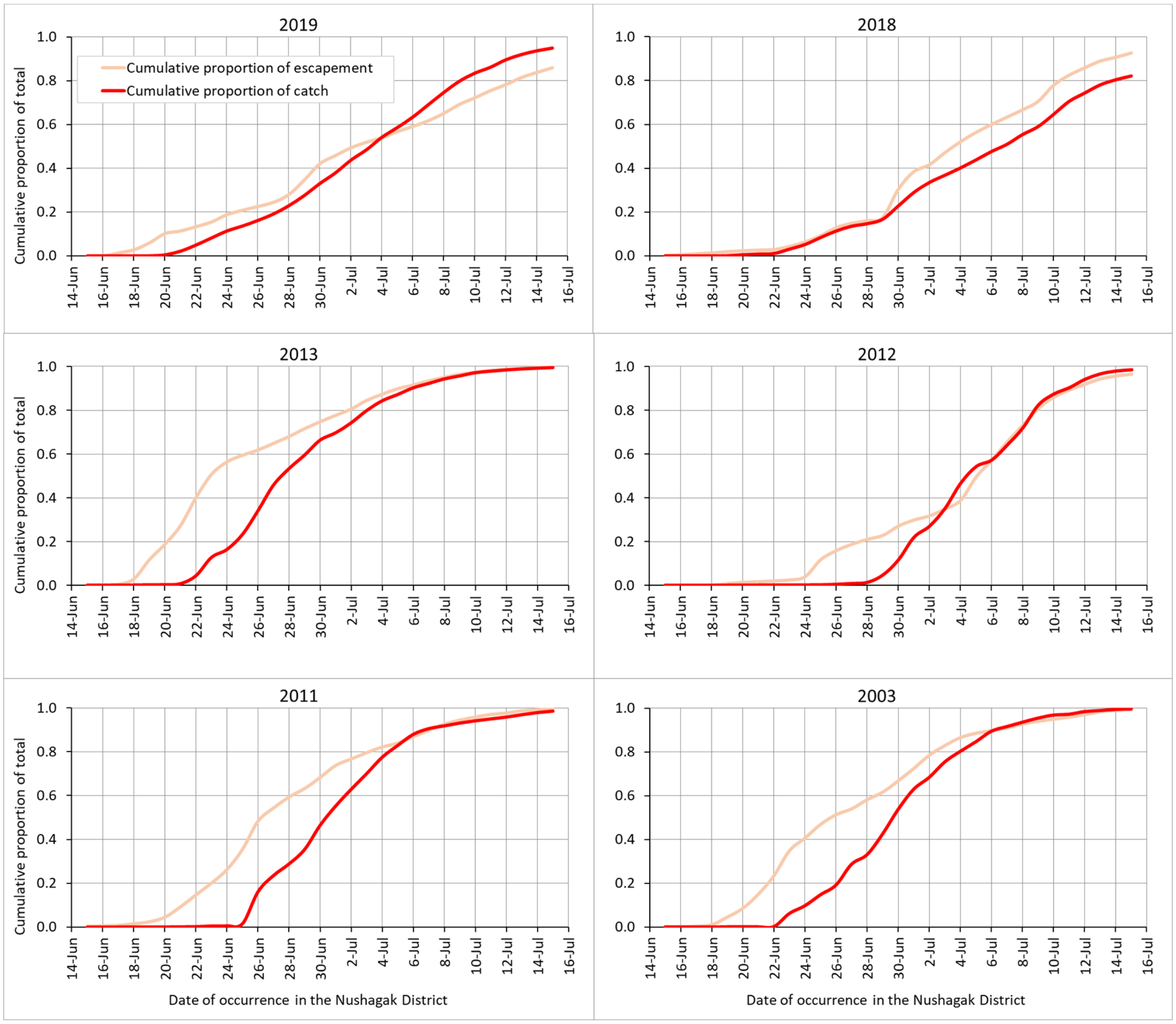

Figure 5. Catch + escapement from Figure 4 converted to cumulative proportions across each season.

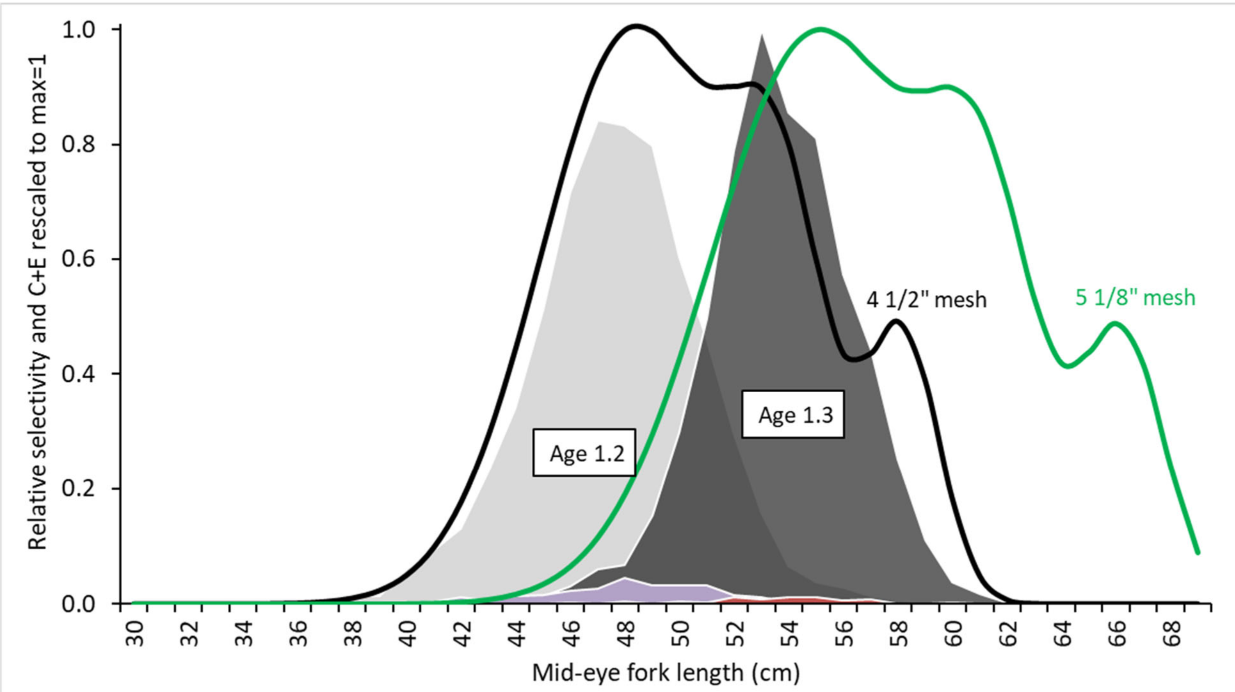

Figure 6. Selectivity curves for 4½” and 5⅛” meshes fished during the 2019 commercial fishery openers (CF protocol) along with length frequency distributions for catch plus escapement (C+E) pooled by each age (note: ages 2.2 and 2.3 are shown as colored area plots but are not labeled). Both selectivity curves and C+E are rescaled to a maximum equal to one.

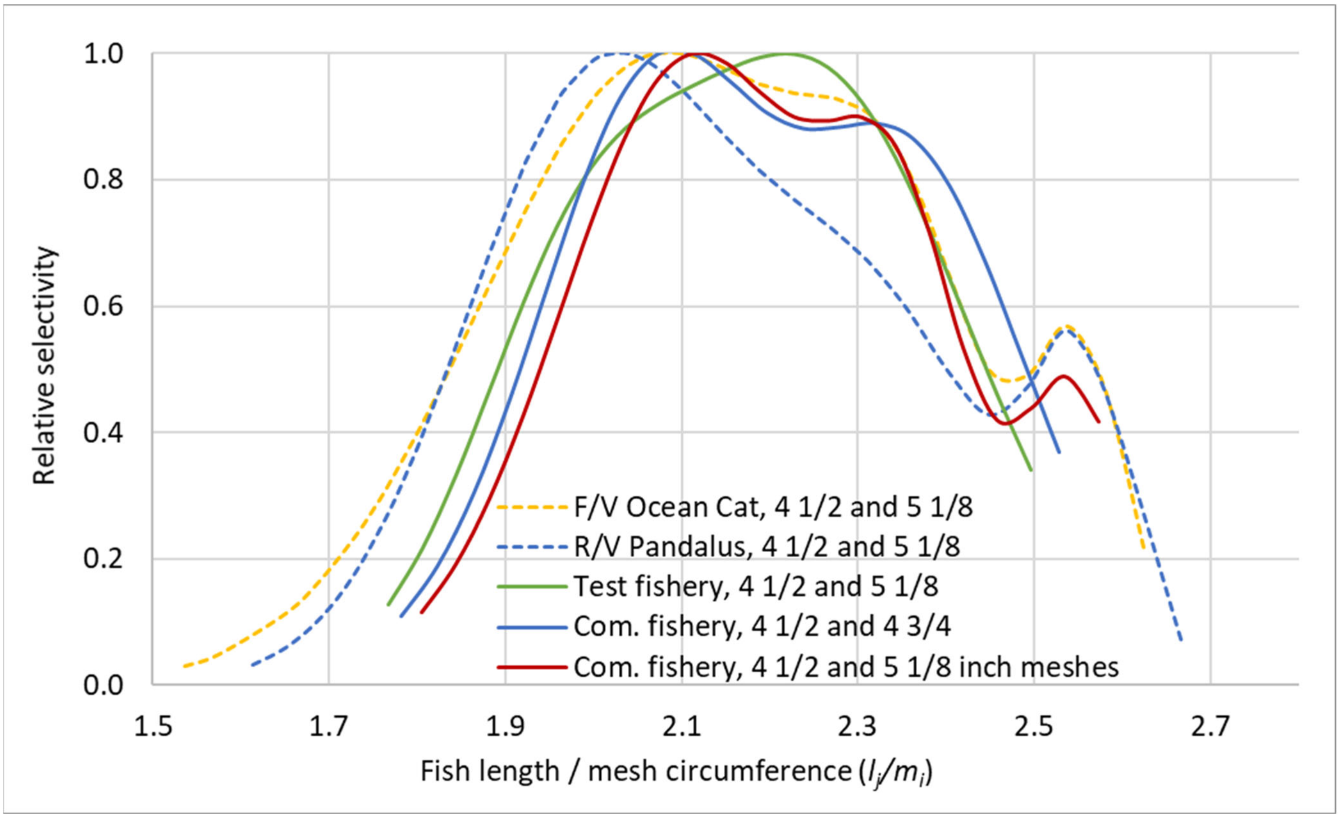

Figure 7. Comparison of selectivity curves developed from various datasets collected in 2019 Nushagak Test Fishery (see Appendix A for methods) along a common axis. Note: sample sizes were too low for the tangle mode to be estimated for the TF and CF 4½"-4¾" mesh curves.

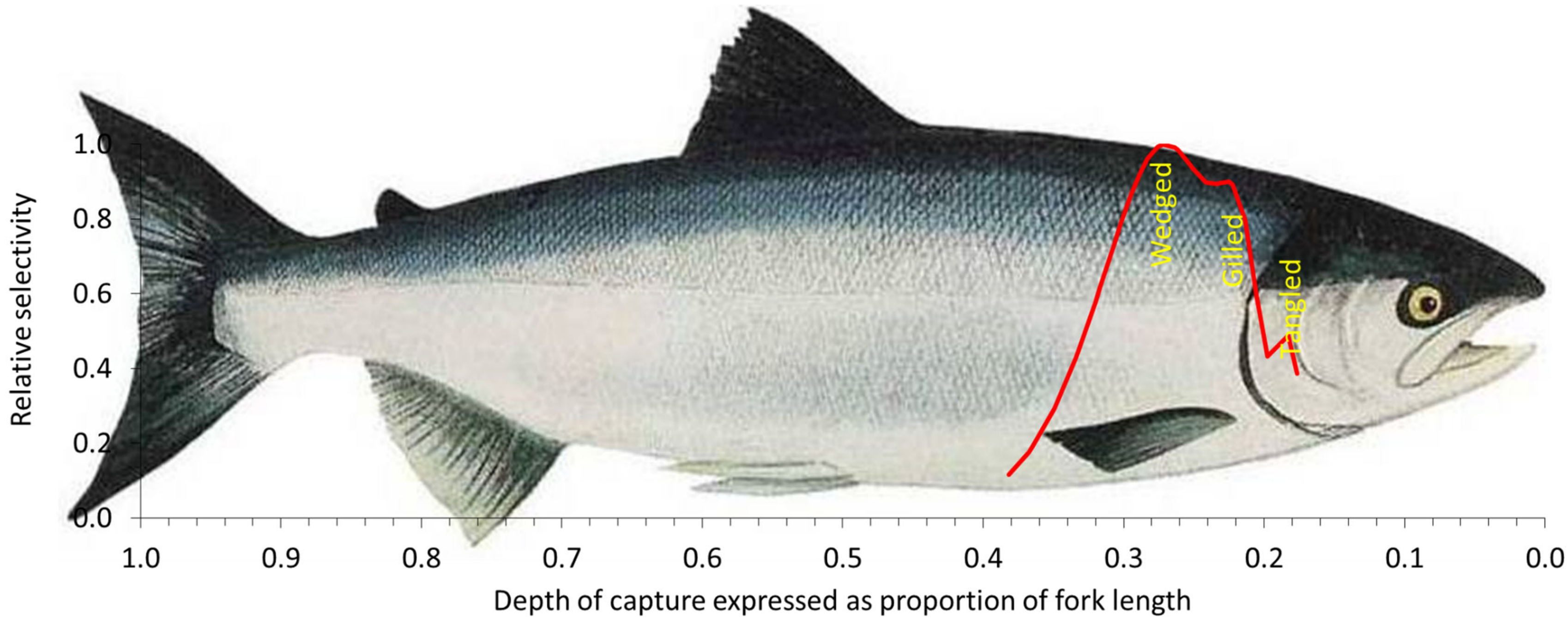

Figure 8. Estimated selectivity curve for 2019 superimposed onto the image of an average shaped oceanic phase Sockeye (image obtained from https://commons.wikimedia.org/wiki/File:Lake_Washington_Ship_Canal_Fish_Ladder_pamphlet_-_ocean_phase_Sockeye.jpg). Starting from right to left three modes aligned with the following body structures: (1) the tangled mode occurred around the pre-operculum; (2) the gilled mode occurred just after the gill cover; (3) the wedged mode occurred between the gill cover and the dorsal insertion.

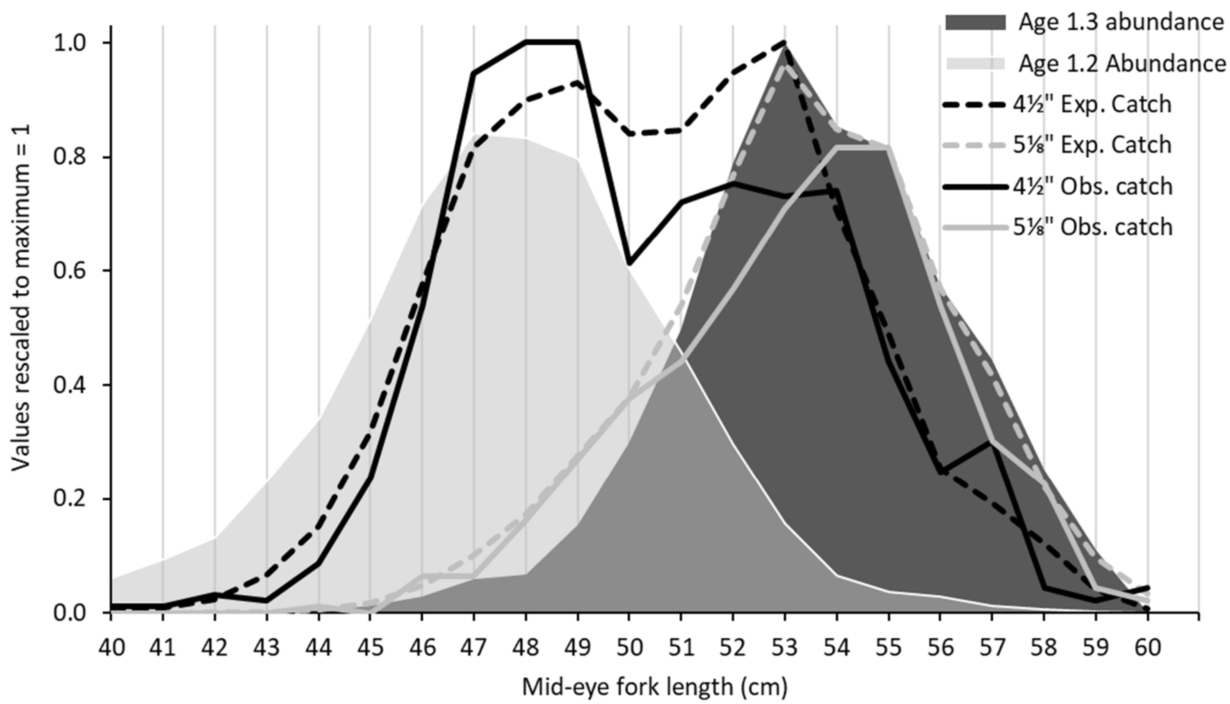

Figure 9. Abundance LFDs of age-1.2 and age 1.3 along with those for test fishery catches observed versus those expected from the estimated selectivity curves for 4½" and 5⅛" meshes fished during the 2019 Nushagak District commercial fishery openers (CF protocol). Note: abundances and catches were respectively rescaled to maximum values equal to one to facilitate comparison.

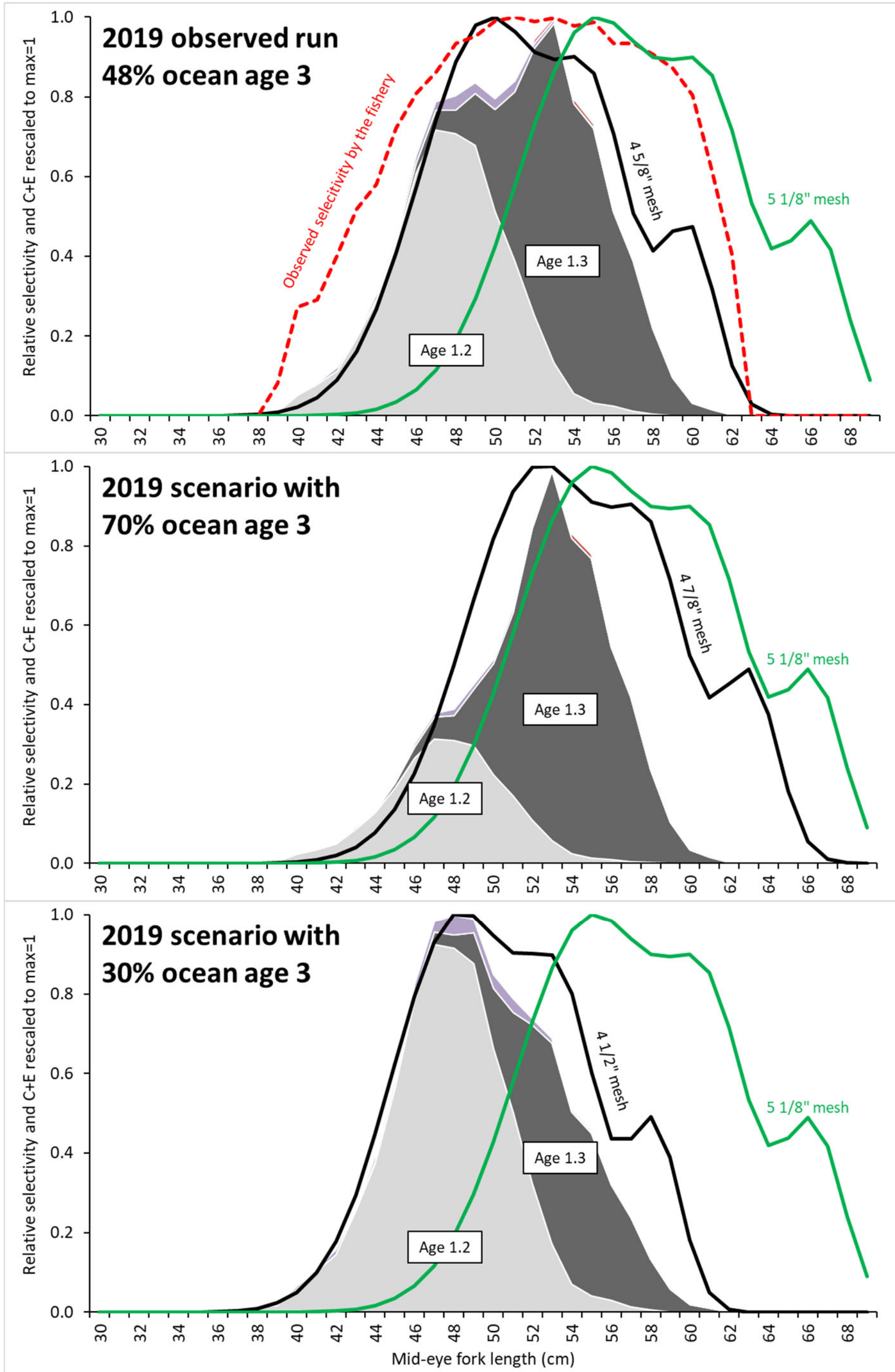

Figure 10. Selectivity curves for the mesh size that maximized the total lbs of catch estimated indirectly (solid lines) for the observed run and for hypothetical scenarios where different ocean ages dominated. Observed selectivity by the fishery (red dashed line) is depicted in the top panel, and the indirect 5⅛" curve is given in all three panels for comparison. Length frequency distributions for catch plus escapement (C+E) pooled by each age (note: ages 2.2 and 2.3 are shown as colored area plots but are not labeled) are also shown. All selectivity curves and C+E are rescaled (max=1).

APPENDIX A: STATISTICAL APPROACH FOR THE ESTIMATION OF GILLNET SIZE SELECTIVITY

Gillnet selectivity is most accurately quantified when the length frequency distribution (LFD) of the population exposed to the gear is known, and the curves can be estimated directly (Millar and Fryer 1999). The catch from each length-mesh size combination is simply divided by the abundance for that length, and the resulting values are rescaled so that the maximum selectivity across all length-mesh size combinations is equal to one. In the Nushagak District, the catch and escapement from the inshore run are sampled for length to provide an estimation of the inshore LFD.

Indirect estimation is based on the relative catches across gear types (in our case two mesh sizes per dataset) and requires, along with other assumptions, that the LFD of the population be estimated simultaneously (Millar and Fryer 1999). Liability from these assumptions aside, the curves represent an estimation of the mesh-specific selectivity for different sized fish that contact the net. Below we expound upon how indirect curves were estimated and verified.

Indirect Estimation of Selectivity

Indirect estimation of selectivity involves comparing relative catches across differing mesh sizes (m_i). Each length was truncated to cm group (l_j); then, catches were summed within each l_j-m_i combination, and sorted by the ratio l_j/m_i. Observed catch for a given ratio, $C(l_j/m_i)$, was the product of inherent selectivity [the proportion of fish contacting the net that are retained=$S(l_j/m_i)$], fish abundance [$d(l_j)$], and fishing intensity [the proportion of $d(l_j)$ that contacted the gear=$q(l_j/m_i)$]:

$$C(l_j/m_i) = S(l_j/m_i) \cdot d(l_j) \cdot q(l_j/m_i) \qquad \text{(A1)}$$

Selectivity was then given by:

$$S(l_j/m_i) = \frac{C(l_j/m_i)}{d(l_j) \cdot q(l_j/m_i)} \qquad \text{(A2)}$$

The shape of the selectivity curve as a function of l_j/m_i can differ across species and researchers of the same species (Hamley 1975). Several shapes defined by models such as normal, lognormal, and bimodal, among others have been used to model selectivity. Popular approaches to indirectly modeling selectivity require this shape to be determined *a priori* (see Millar and Fryer 1999 for a review). We chose the algorithm developed by Tang et al. (2010) for estimating selectivity indirectly because unlike these approaches, no predetermined shape was necessary. Instead, the relative abundance of fish in each length group was estimated and used to adjust catches across all lengths to what would have been caught had all lengths been equally represented. The adjusted catches revealed the shape of the selectivity curve allowing the choice of selectivity curve shape to be more informed. The steps for using this approach can be visualized in Figure A1 and were as follows:

1. The relative heights of $C(l_j/m_i)$ plotted against l_j/m_i were influenced by changes in selectivity $S(l_j/m_i)$ along the range of l_j/m_i values, as well as changes in contact abundance [$d(l_j) \cdot q(l_j/m_i)$]. The influences of abundance and fishing intensity on contact abundance (termed "relative abundance" by Tang e t al. 2010) were confounded and could not be separated just based on relative catches across mesh sizes without extraneous information about $d(l_j)$ from knowing the population LFD (Millar and Fryer 1999). Thus, we had to assume constant fishing intensities, $q(l_j/m_i)$=1; i.e., contact abundance was the same as fish abundance.

2. Tang et al. (2010) argued that differences in $C(l_j/m_i)$ points adjacent on the x-axis were mostly due to varying contact abundances; points further apart on the x-axis were due to both varying contact abundances as well as differences in selectivity. Their idea was to reduce the vertical distances between adjacent points by adjusting contact abundance for each l_j. When $d(l_j)$=1 the unadjusted selectivities, $S(l_j/m_i)$, were the same as $C(l_j/m_i)$. When $d(l_j)$>1, the adjusted selectivities, $S_{adj}(l_j/m_i)$ were as follows:

   $$S_{adj}(l_j/m_i) = C(l_j/m_i)/d(l_j) \quad \text{(A3)}$$

   Values of $d(l_j)$ were adjusted for each l_j to minimize the following objective function:

   $$ObjFunc = \sum_k \left\{ \left(S_{adj}(l_j/m_i)_k - S_{adj}(l_j/m_i)_{k+1}\right)^2 \cdot min\left(C(l_j/m_i)_k, C(l_j/m_i)_{k+1}\right) \right\} \quad \text{(A4)}$$

   where, k=the ordered rank from the sorted list of l_j/m_i.

3. The resulting values of $S_{adj}(l_j/m_i)$ were then smoothed by fitting an appropriate curve. Tang et al. (2010) discovered the bimodal curve, commonly found in the selectivity literature, produced the best fit to the resulting shape of $S_{adj}(l_j/m_i)$ for Pink Salmon *O. gorbuscha*. Our resulting curves revealed selectivity to be more nuanced requiring a trimodal curve, which we fit assuming additive error.

The model fitting algorithm intrinsically estimated the LFD of the fish exposed to the test fishery; thus, no *a priori* distribution was assumed. Assumptions regarding the estimation of selectivity curves include (1) the relationship between girth and length was linear, (2) equal fishing intensity across mesh sizes, (3) equal fishing intensity across fish sizes available to the gear, and (4) equal availability across fish sizes. The first assumption allows for the shapes of the mesh specific selectivity curves to be identical. Assumptions 2 and 3 are required for their heights to be identical as well.

Equal fishing intensity across mesh sizes requires that the same proportion of the size-specific population encountered each mesh (violation could come from one mesh being avoided more than the other or conversely saturated). Equal fishing intensity across fish lengths means that fish contacted the gear in proportion to their relative abundance across lengths of fish available to the gear (violation could come from larger fish swimming faster or exhibiting a greater rate of net avoidance).

We found that most of the literature describing the indirect estimation of selectivity combined Assumptions 1-3 into a single assumption called the principle of geometric similarity, first described by Baranov (1914), but then parse violations to this principle into allometric growth or mechanisms that cause differential fishing intensities across gears and fish sizes (e.g., Millar and Fryer 1999). Our delineation of assumptions coincides with the types of indirect curves introduced below.

Millar and Fryer (1999) define three selectivity curves differing in the subset of the fish population to which they apply: (1) the population-selectivity curve quantifies the probability that any fish in the population of given length will be captured by the gear and allows for the difference between LFDs for the population and the catch to be estimated; (2) the available-selectivity curve quantifies the probability that a fish of given length will be captured given it was available to the gear; and (3) the contact-selectivity curve quantifies the probability that a fish of given length will be captured given that it contacted the gear.

The data rendered from the experimental fishing at in the Nushagak test fishery allowed for parameterization of contact-selectivity curves given Assumptions 1 and 2 were met. The resulting curve would look the same regardless of whether Assumptions 3 and 4 were met as the algorithm does not distinguish between whether a fish of a given size (l_i) was more abundant or more available (Millar and Fryer 1999). The implications of meeting Assumptions 3 and 4 affects how the curves can be used. A contact-selectivity curve can be used to identify which fish length and/or age each mesh size selects for the most. Meeting Assumptions 3 and 4 would allow their use as population-selectivity curves, which is required if the catch LFD is to be corrected to represent that for the population. The selectivity literature is often unclear about which type curve is being estimated (Hamley 1975; Millar and Fryer 1999).

Verification of the Selectivity Curves

Comparison of observed and predicted LFDs for test fishery catches.—Mesh-specific length frequency distributions (LFDs) for test fishery catches can be predicted by applying the estimated selectivity curves to the known LFD for the entire run. Assuming the test fishery was exposed to fish with a LFD representative of the entire run, within each mesh the observed and predicted catch LFD shapes and heights should be similar. Violating any of Assumptions 1-4 would cause them to differ. Thus, we performed this analysis to help delineate the direction and magnitude of any bias in the selectivity curves.

Comparison to anatomical features. —Following the 2012 season, we noticed the estimated shape of the selectivity curves varied slightly among years at Port Moller. Reasons for the variability could have come from violation of Assumptions 1 or 2. To assess the shape of our curves relative to the anatomical features of a Sockeye salmon, we collected data in 2013 that allowed curves to be superimposed over a typical specimen. From a random sample collected throughout the season, we measured the distance from the tip of the snout to the net mark (depth of capture; DOC), along with fork length (FL), MEFL (l_j), and mesh size (m_i). Depth-of-capture was then expressed as a proportion of FL (DOC/FL) and plotted against l_j/m_i to parameterize the following model:

$$\frac{DOC}{FL} = \alpha \cdot \left(l_j/m_i\right)^{\beta} \qquad \text{(A5)}$$

where, α and β are intercept and slope parameters for the power curve. This model was used to convert each l_j and m_i combination to corresponding DOC/FL values (Figure A2). The indirectly estimated selectivity curve was plotted against the estimated DOC/FL values and superimposed over an image of a typical Sockeye in its oceanic phase (https://commons.wikimedia.org/wiki/File:Lake_Washington_Ship_Canal_Fish_Ladder_pamphlet_-_ocean_phase_Sockeye.jpg). The x-axis was rescaled so that from right to left a value of zero occurred at the tip of the snout, and a value of one occurred at the fork of the tail (Figure 8 in the body of the this report).

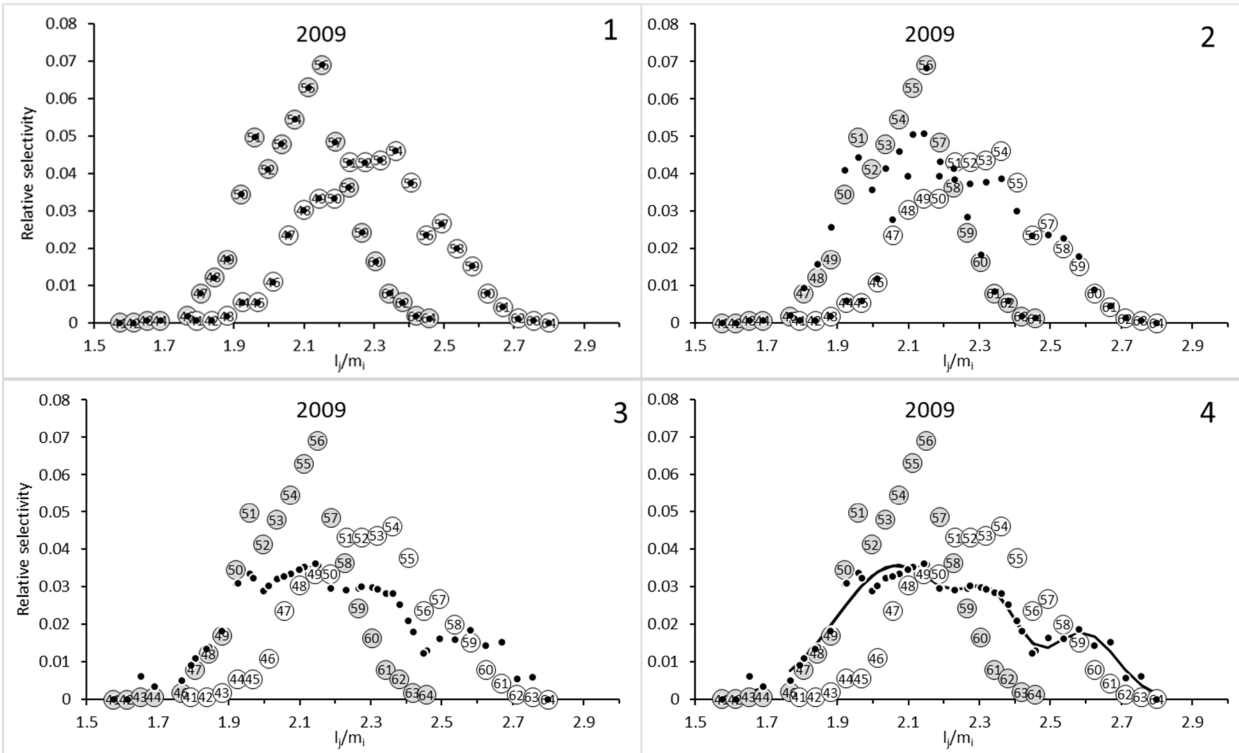

Figure A1. (1) $S(l_j/m_i)$ or $C(l_j/m_i)$ as a function of fish length/mesh size (l_j/m_i); shaded circles represent catches from 4½” mesh, white circles 5⅛” mesh (cm group is indicated within each). (2) $S_{adj}(l_j/m_i)$ shown as black dots midway during the adjustment algorithm. (3) $S_{adj}(l_j/m_i)$ for the final conversion with black dots representing the observed selectivity curve. (4) The observed selectivity curve smoothed with a trimodal curve. These data were collected from the 2009 Port Moller Test Fishery.

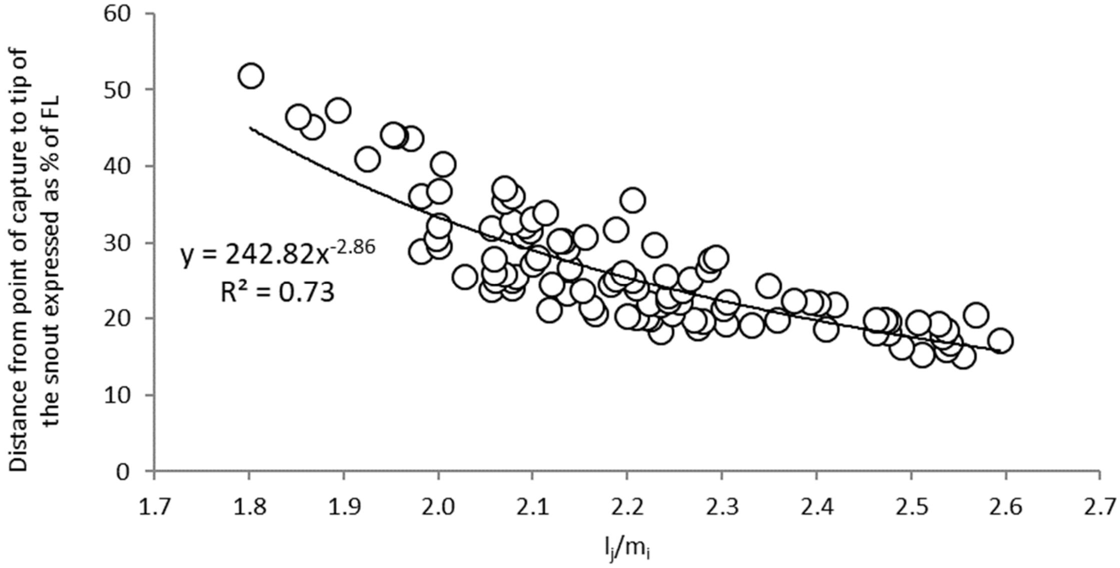

Figure A2. Depth of capture versus l_j/m_i ratio collected in 2013. Values are expressed as a percent of fork length (FL).

APPENDIX B: RESULTS FROM THE NUSHAGAK DISTRICT TEST FISHERY, 2020

Similar to 2019, a Nushagak District test fishery was again operated in 2020. The objectives and methods were identical to those for the previous year and are detailed in the body of this report. The primary purpose of this endeavor was again to provide daily information to the area management biologist (Tim Sands) regarding the buildup of fish in the district early in the season before they enter their natal river systems. In addition, length data from fish captured in the test net were used to characterize the size selectivity of gillnets across a range of mesh sizes. Below, we update selected tables and figures used to present the 2019 results.

A total of 70 sets were made in the Nushagak District during June 16 to July 2 resulting in a total catch of 1,782 Sockeye; 85% or 1,508 fish were measured for length. Unlike 2019, only one net configuration was used based on the 2019 recommendation that the 150-fathom net comprised of six 25 fathom shackles alternating in mesh sizes (4½" and 5⅛") was optimum for our research purposes.

Test Fishing to Detect Fish Abundance in the Nushagak District

Test fishing (sets using the TF protocol) occurred for eight days (June 16-June 24) prior to the first commercial fishing opener on June 25; six more TF protocol sets happened during June 25-July 2 after an opener had closed on those dates. Selection of station locations was again exploratory in nature, but more evenly distributed throughout the eastside of the District compared to 2019 (Figure B1). Nevertheless, test fishing CPUE did appear to track the buildup of fish in the District during June 16-June 24 (Figure B2, top panel). The ratio of Sockeye:Chinook estimated from the test fishery catches off a bit in magnitude as compared to this ratio estimated for the reconstructed runs in the District (Figure B2, bottom panel). Nevertheless, spikes in this ratio from the test catches and the reconstructed runs seemed to align. The crew tried for 30-40 min mean fishing times (MFTs) and averaged 40 min.

After June 25, high commercial fishing effort (overall exploitation rate=0.70) was used to prevent/minimize over-escapement into the three systems from a total Nushagak District run of 13 million Sockeye. As in 2019, the manager attempted to spread escapement across the entirety of the season in proportion to the run (daily exploitation rate range=0.54-0.85).

Selectivity Curves for the Nushagak District

Fewer fish were sampled during the 2020 test fishery compared to 2019. Throughout the season, the two fishing protocols used, TF and CF, produced 992 and 516 length measurements. For selectivity curve estimation, we chose to pool these data to increase sample size. Note: these data were front-loaded in that 81% of the C+E occurred after the last test fishing date (July 2).

Even if the first ~20% of the run to which the test fishery was exposed misrepresented the run's overall LFD, unbiased contact selectivity curves can still be estimated. First, the 2020 selectivity curve was very similar to the 2019 curve (Figure B3), for which strong evidence against bias was provided. Consequently, the modes on the 2020 selectivity curve line up with the three mechanisms of gillnet capture (not shown for 2020 but see Figure 8 in the body of this report). This finding agrees with observations of where along the body fish are mostly likely to be caught and suggest that the location and relative heights of these modes as estimated with the indirect contact selectivity curves were reasonable for 2020.

We applied the 4½" and 5⅛" mesh selectivity curves to the observed 2020 length frequency distribution (LFD) for the entire Nushagak District abundance to predict catch percentages for the meshes. We then compared these percentages to what was observed in both the TF and CF protocols (Table B1). During openers when the CF protocol was used, we observed that 73% of the catch came from the 4½" mesh—nine percentage points greater than our prediction of 64%. During closures when the TF protocol was used, the observed percentage was closer (70%), but still six percentage points greater than the predicted 64%. The phenomenon of larger fish being filtered by the fishery would have to have occurred at a greater rate as compared to 2019 to completely explain the TF-CF catch percentage difference in 2020. Alternately, the fact that six of the TF sets occurred on days immediately following a commercial opener likely caused these samples to come from a somewhat filtered population as well.

Comparing observed and expected catch LFDs for the CF protocol to the age-specific abundance LFDs illustrates this point further (Figure B4). The observed and predicted catch LFDs for both meshes match somewhat over the predominant age-1.2 sizes (bins ≤ 49 cm), but observed catches become less over cm bins ≥ 50 cm that cover the majority of age 1.3 abundance. These results further indicate that test fishery catches came from a passing abundance biased towards age-1.2 fish as compared to the observed overall run's age composition.

Optimizing Selectivity Curves for the Nushagak District

Once the shape of the selectivity curve along the l_j/m_i axis was estimated based on the CF 4½"-5⅛" dataset, a curve for any mesh size could be approximated (i.e., in addition to the two meshes used to estimate the curve). The observed size selectivity by the fishery appeared to be dome shaped and more consistent across a wider range of sizes than any particular individual mesh size (Figure B5). Across all fishermen, a range of mesh sizes was used which explains why this observed pattern occurred. Nevertheless, we approximated an average single mesh size used by the fishery (about 4⅝") while simultaneously adjusting the exploitation rate so that simulated catches for each age matched those observed. Then, holding this adjustment constant we changed mesh size from 4½" to 5⅛" by ⅛" increments and report the hypothetical performance of three objective functions: (1) maximize total catch, (2) maximize total lbs of catch, and (3) equalize exploitation rates across ages (Table 4).

The observed run was 63% 2-ocean and 37% 3-ocean sockeye. As predicted by the simulated run dominated by 2-ocean fish for the 2019 data (70% 2-ocean; Table 4 in the body of this report), the mesh size that maximized total catch, total lbs of catch, and equalized exploitation rates was estimated to be 4½" (Table B2). Furthermore, the 5⅛" mesh performed poorly in these regards, again as predicted by the 2019 simulated run of 70% 2-ocean fish. In spite of the predominant use of this mesh size historically, there is reason to believe that fishermen are adapting. The 2018 Nushagak District run was the greatest on record (34 million) to which an above average exploitation rate was applied by the fleet (Figure B6, top panel). The following year (2019; 18 million), the exploitation rate was even greater and was spread more evenly across a broader range of sizes (Figure B6, bottom panel). Exploitation was lower for 2020 due to a smaller run size (13 million) but remained more evenly distributed across sizes. On explanation could be that a larger portion of the fleet is shifting to smaller mesh sizes. Due to the shape of the estimated selectivity curve (Figure B5), this occurrence would harvest more smaller fish without foregoing larger fish thereby flattening the selectivity curve for the fleet in general.

Table B1. Observed and predicted (from the selectivity curves) catch percentages between various mesh pairings used in the 2020 test fishing net for the Nushagak District.

Protocol	Meshes fished (inches)	Obs. % of catch from 4½" mesh	Pred. % of catch from 4½" mesh
CF	4 1/2-5 1/8	73%	64%
TF	4 1/2-5 1/8	70%	

Table B2. Estimated catch metrics across various mesh sizes from the selectivity curve based on the CF and TF 4½”-5⅛” dataset collected in the Nushagak District during 2020. Shaded values indicate optimized values.

Mesh size (inches)	Catch (individuals)	Fish wt. (lbs)	Catch (lbs)	Exploitation rate		Efficiency relative to mesh that max. lbs
				Age 1.2	Age 1.3	
Observed run with 37% ocean age 3 fish						
4 1/2	8,494,759	4.17	35,450,599	0.69	0.69	1.00
4 5/8	8,166,642	4.31	35,196,456	0.60	0.76	0.99
4 3/4	7,553,025	4.45	33,647,056	0.50	0.80	0.95
4 7/8	6,681,499	4.60	30,723,667	0.40	0.79	0.87
5	5,714,009	4.74	27,079,030	0.30	0.74	0.76
5 1/8	4,715,850	4.88	23,007,185	0.21	0.67	0.65

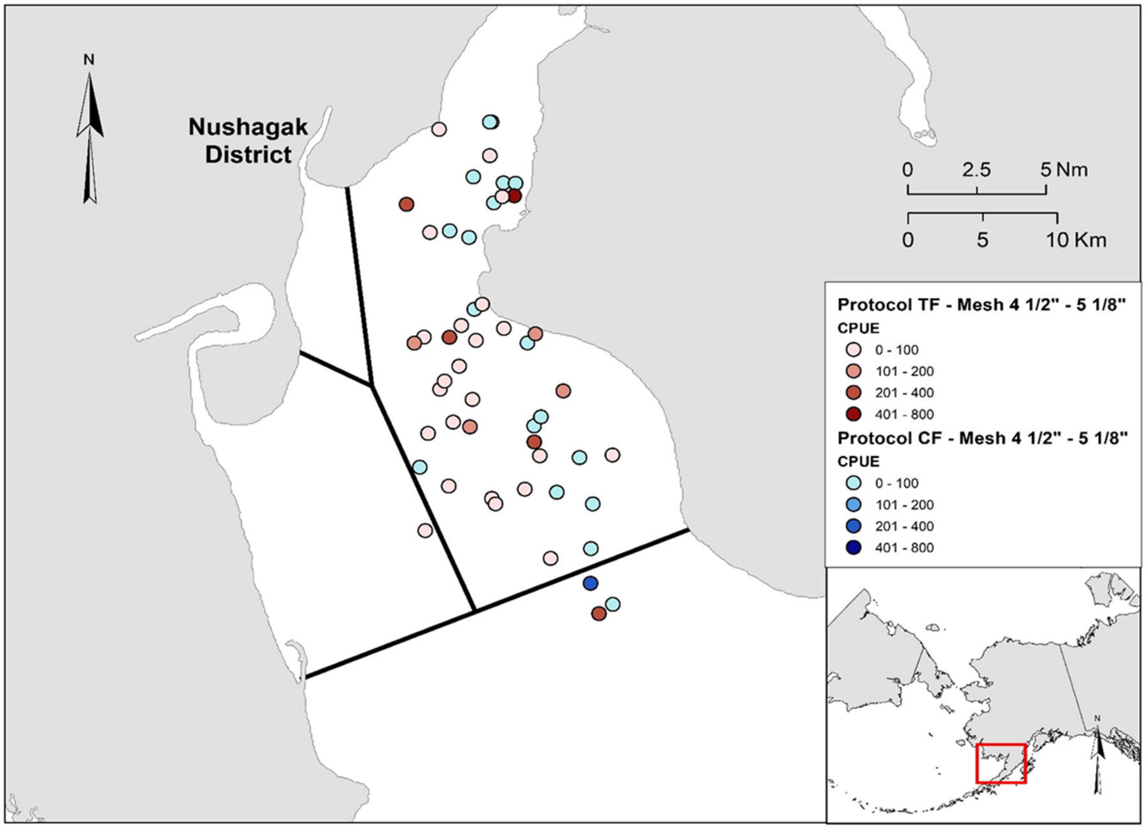

Figure B1. Location of stations fished during each fishing protocol/mesh size configuration combination. Intensity of color reflects greater catch-per-unit-effort (CPUE=number of Sockeye caught if a 200-fathom net had been fished for one hour).

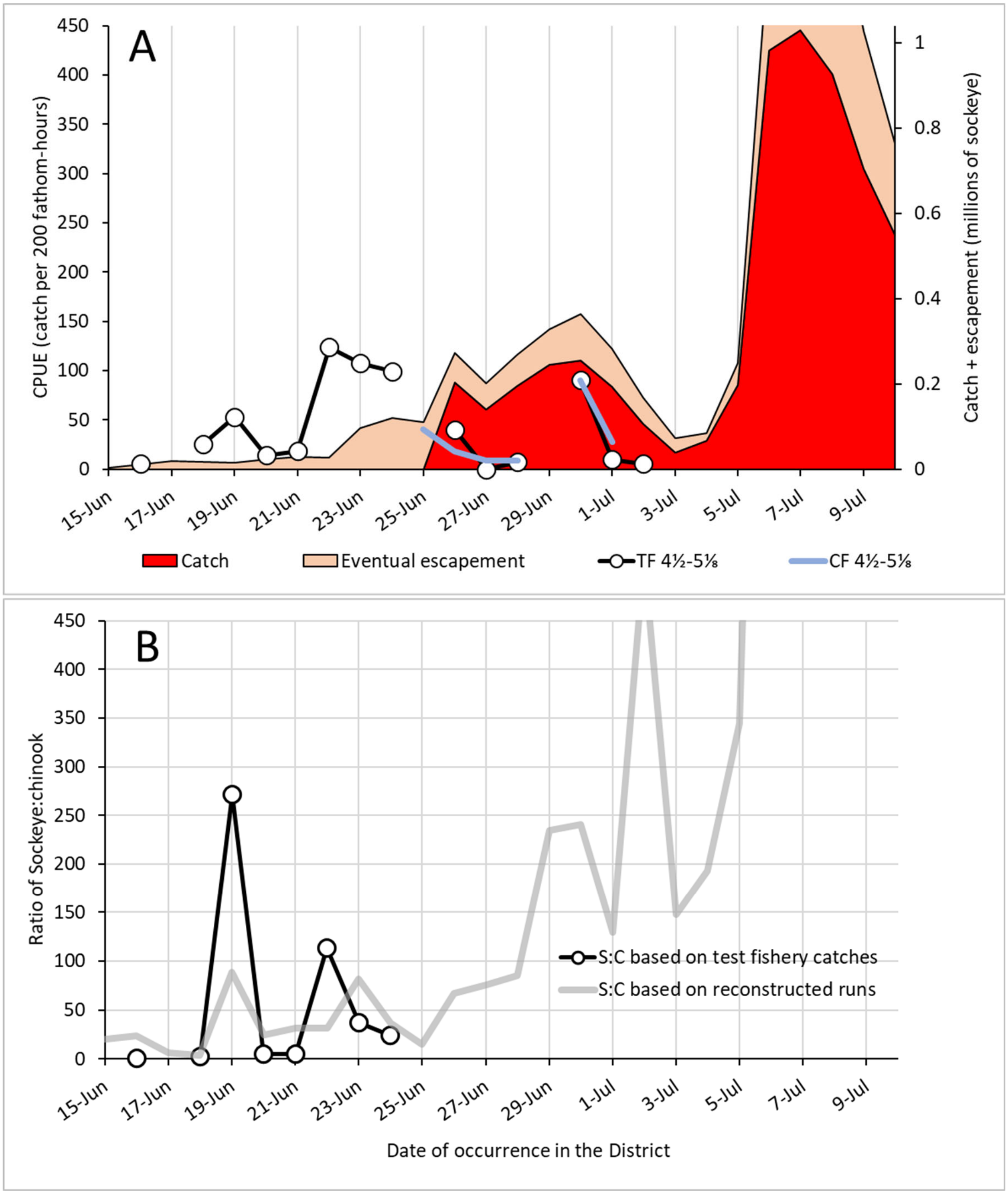

Figure B2. Test fishing indices. (A) CPUE (left y-axis) and catch + escapement (right y-axis) in the Nushagak District during 2020. Fishing by the test boat during closures is indicated by "TF" and "CF" during openers. The X-axis represents the date of occurrence in the district; thus, the escapement values depicted were combined from all three systems (Wood, Nushagak, and Igushik), each lagged back to the district by a number of days that varied across systems. (B) The ratio of Sockeye:Chinook in the TF catches versus that for the reconstructed runs.

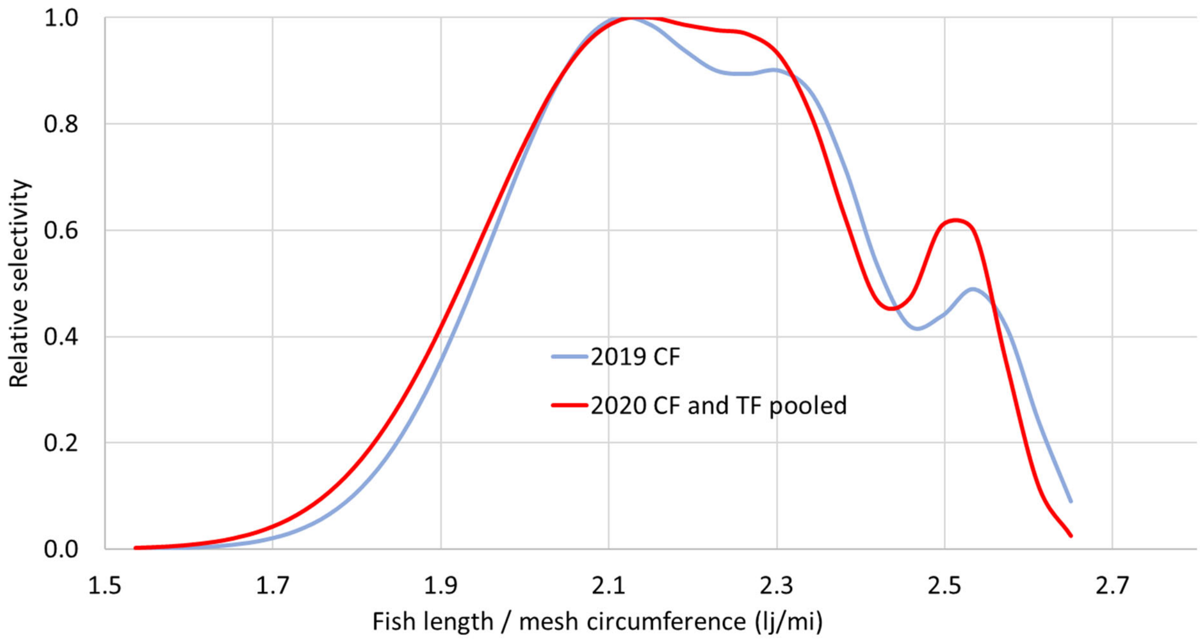

Figure B3. Comparison of 2019 and 2020 selectivity curves developed from the Nushagak Test Fishery (see Appendix A for methods) along a common axis.

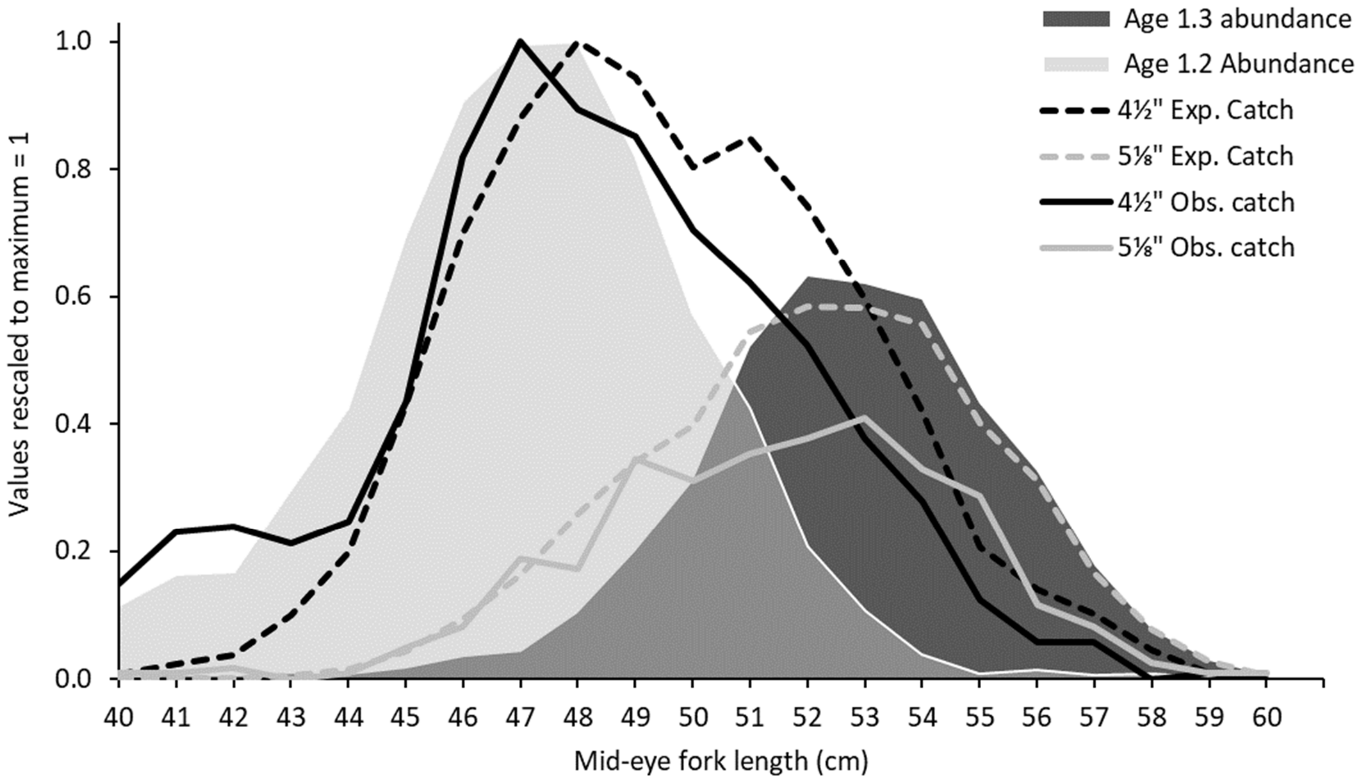

Figure B4. Abundance LFDs of age-1.2 and age 1.3 along with those for test fishery catches observed versus those expected from the estimated selectivity curves for 4½" and 5⅛" meshes fished during 2020. Note: abundances and catches were respectively rescaled to a maximum value equal to one to facilitate comparison.

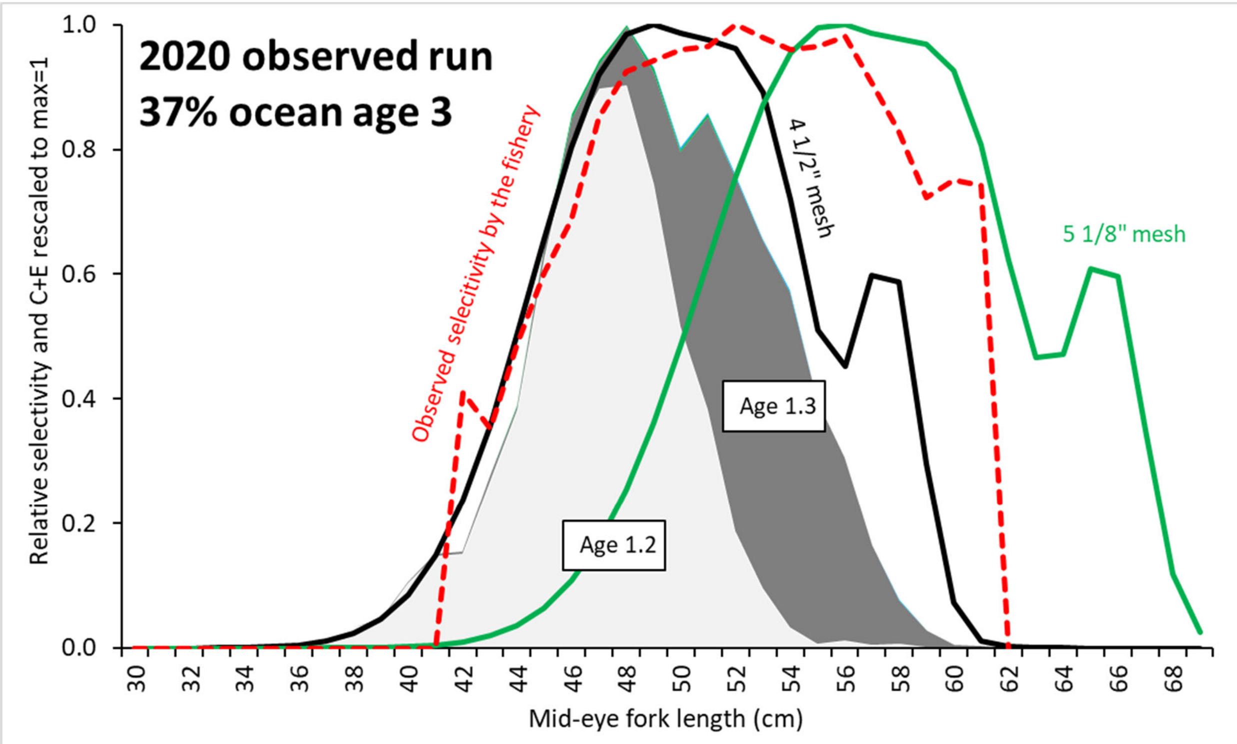

Figure B5. Selectivity curves for the mesh size that maximized the total lbs of catch estimated indirectly (solid lines) for the observed run. Observed selectivity by the fishery (red dashed line), and the indirect 5⅛" curve is given for comparison. Length frequency distributions for catch plus escapement (C+E) pooled by each age (note: ages 2.2 and 2.3 are shown as colored area plots but are not labeled) are also shown. All selectivity curves and C+E are rescaled (max=1).

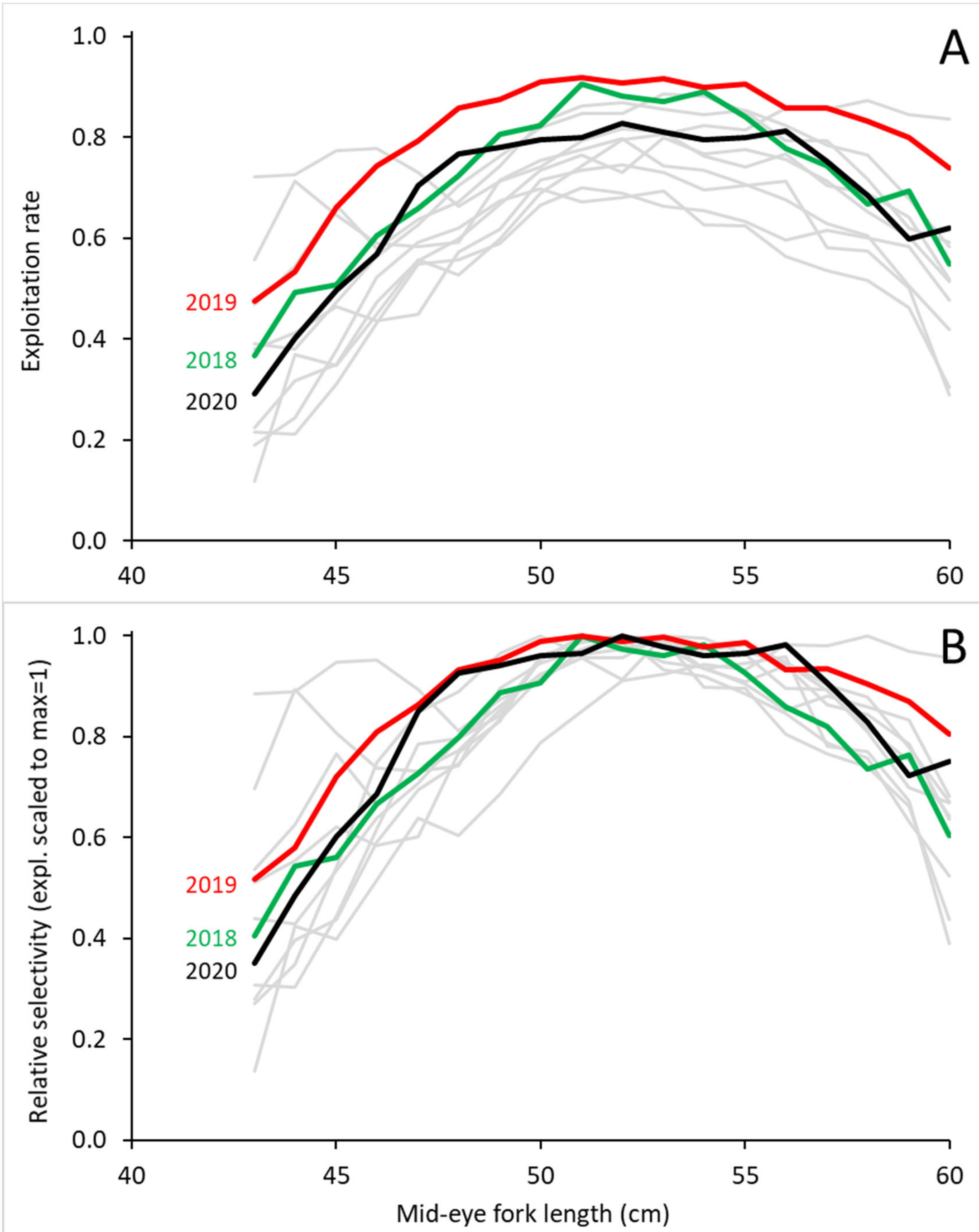

Figure B6. (A) Observed commercial fishing exploitation in the Nushagak District fishery (2009-2020) by fish size (cm bins). (B) Exploitation rescaled to a maximum value equal to one, which equates to relative selectivity across fish sizes by the overall fleet.